Pesticide-induced resurgence in brown planthoppers is mediated by action on a suite of genes that promote juvenile hormone biosynthesis and female fecundity

Yang Gao[a,1], Shao-Cong Su[a,1], Ji-Yang Xing[a,1], Zhao-Yu Liu[a], Dick R. Nässel[b], Chris Bass[c], Cong-Fen Gao[a], Shun-Fan Wu[a,*]

[a] College of Plant Protection, Nanjing Agricultural University, Nanjing 210095, China.

[b] Department of Zoology, Stockholm University, Stockholm, Sweden

[c] College of Life and Environmental Sciences, Biosciences, University of Exeter, Penryn Campus, Penryn, UK

[1] These authors contributed equally to this work.

*Corresponding author. E-mail address: wusf@njau.edu.cn (S.-F. Wu)

Abstract

Pesticide-induced resurgence, increases in pest insect populations following pesticide application, is a serious threat to the sustainable control of many highly damaging crop pests. Resurgence can result from pesticide-enhanced pest reproduction, however, the molecular mechanisms mediating this process remain unresolved. Here we show that brown planthopper (BPH) resurgence in rice crops following exposure to sublethal doses of the pesticide emamectin benzoate (EB) results from the coordinated action of a suite of genes that regulate juvenile hormone (JH) levels, resulting in increased JH titer in adult females and enhanced fecundity. We demonstrate that EB treatment at sublethal levels results in profound changes in female BPH fitness including increased egg maturation and oviposition. This enhanced reproductive fitness results from the EB-mediated upregulation of key genes involved in the regulation of JH, including *JHAMT and Kr-h1* and the downregulation of allatostatin (*AstA*) and allatostatin receptor (*AstAR*) expression. AstA signaling is known to inhibit the production of JH in the corpora allata and hence EB exposure diminishes this inhibitory action. We find that the changes in gene expression following EB exposure are caused by the allosteric action of this insecticide on its molecular target, the glutamate-gated chloride channel (GluClα). Collectively, these results provide mechanistic insights into the regulation of negative pesticide-induced responses in insects and reveal some key actors involved in the JH-signaling pathway that underpin pesticide resurgence.

Keywords: resurgence; reproduction; pesticide; allatostatin; brown planthopper

Significance

Pesticides remain a key means of controlling many of the world's insect pests. However, in some cases, pesticide applications can result in resurgence of pest populations due to pesticide-induced increases in fecundity. In the current study, we show that pesticide resurgence in the brown planthopper (BPH) following exposure to the insecticide emamectin benzoate (EB) results from the transcriptional reprogramming of a diverse suite of positive and negative regulators of juvenile hormone (JH), a critical regulator of insect development and reproduction. This in turn leads to profound increases in female BPH reproductive fitness and enhanced fecundity. Our findings unravel some of the molecular mechanisms mediating pesticide-induced pest resurgence and inform the development of novel strategies to control highly damaging crop pests.

Introduction

Chemical pesticides remain the primary means of controlling many of the world's most damaging arthropod crop pests (Janssen and van Rijn, 2021; Wu et al., 2018a). However, pesticide applications can result in pest resurgence, increases in pest insect populations that exceed natural, untreated population sizes, following an initial reduction of the pest population (Gandara et al., 2024; Guedes et al., 2016; Hardin et al., 1995; Wu et al., 2020). Two mechanisms have been implicated in pest resurgence - the loss of beneficial insects including natural enemies, and pesticide-enhanced reproduction in the pest insect (Wu et al., 2020). In the case of the latter, several pesticides, such as the insecticides triazophos, deltamethrin and the fungicide jinggangmycin, have been reported to stimulate reproduction in pest insects (Ge et al., 2010; Wu et al., 2018b; Zhang et al., 2014). Pesticide-enhanced pest reproduction has been linked to changes in the physiology and biochemistry of pest organisms after exposure to pesticides (Guedes et al., 2016; Wu et al., 2020). However, the molecular mechanisms underlying enhanced reproduction associated with pest resurgence remain poorly resolved.

The brown planthopper (BPH), *Nilaparvata lugens* (Stål), is a notorious pest of rice crops throughout Asia causing annual losses of ~300 million dollars across major rice producing countries (Wu et al., 2020; Wu et al., 2018a). BPH inhibit the growth of rice plants by feeding on the phloem, and also transmit highly damaging plant viruses including rice grassy stunt virus and rice ragged stunt virus (Sōgawa, 1982). Currently, chemical insecticides play an indispensable role in the control of BPH due to their efficiency, rapid effect, and low cost. However, due to the widespread and intensive

use of chemical insecticides, BPH has developed resistance to the majority of compounds used for control (Wu et al., 2018a; Zeng et al., 2023).

Emamectin benzoate (EB) and abamectin are avermectin pesticides, and act as allosteric modulators of insect glutamate gated chloride channels (GluClα) (Wolstenholme, 2012), thereby inhibiting muscle contractions that lead to the cessation of insect feeding and subsequent death (Ishaaya et al., 2002). These insecticides exhibit particularly strong effect against Lepidoptera such as the rice leaffolder, *Cnaphalocrocis medinalis* Guénee, an important foliage-feeding insect which attacks rice during the vegetative stage (Chintalapati et al., 2016). Both BPH and the rice leaffolder are migratory pests with overlapping migratory paths, however, their occurrence period in the field differs by approximately one month, with leaffolders appearing earlier than BPH. Therefore, the use of EB to control rice leaffolder has the potential to impact BPH arriving later, via exposure to sublethal concentrations of this compound. It has been observed that when farmers use EB and abamectin to control leaffolders on rice crops in China, BPH outbreaks frequently occur in the same field. While sublethal doses of certain pesticides have been shown to enhance fecundity in BPH, including the insecticides triazophos and deltamethrin (Ge et al., 2013; Ge et al., 2010; Zhang et al., 2014; Zhang et al., 2022b) and the fungicides carbendazim and jinggangmycin (Wu et al., 2018b), whether avermectins trigger resurgence in BPH via insecticide-enhanced reproduction remains unclear.

Reproduction in insects is influenced by external factors such as light (Wang et al., 2021), temperature (Meiselman et al., 2022), humidity (Roy et al., 2015) and nutrition

(Smykal and Raikhel, 2015), as well as endogenous factors such as juvenile hormone (JH) (Santos et al., 2019), ecdysone (Hun et al., 2022), insulin- (Ling and Raikhel, 2018) and target of rapamycin (TOR) signaling pathways (Ahmed et al., 2020; Badisco et al., 2013; Du et al., 2022; Lu et al., 2016). Of these, JH has been particularly implicated in insecticide-induced enhanced fecundity, with triazophos and deltamethrin treatments leading to increased circulating JH III titers in BPH females (Wu et al., 2020). JH is synthesized and secreted by the corpora allata in insects (Luo et al., 2021), and promotes reproduction by regulating the biosynthesis and secretion of vitellogenin (Vg) in the female fat body, and stimulating the absorption of Vg by the developing oocytes (Santos et al., 2019). However, the regulation of JH is complex (Riddiford, 2008; Santos et al., 2019) and the key actors involved in JH-mediated pesticide-enhanced reproduction remain to be resolved. Previous findings reported that the GluCl receptor is involved in JH biosynthesis in cockroaches (Chiang et al., 2002a; Chiang et al., 2002b; Liu et al., 2005). However, it is still unknown whether insecticides that target the GluClα can increase reproduction in pest insects and the mechanisms by which GluClα receptors regulate JH production remain to be unraveled.

In this study, we used a range of approaches to investigate the impact of sublethal doses of avermectins on BPH fecundity, and unravel the molecular mechanisms mediating enhanced reproduction following exposure to this insecticide class. We show that avermectin exposure results in profound changes in the expression of a key suite of genes that in combination regulate JH, which results in increased JH titer in adult females, which promotes fecundity. Interestingly, we found

that emamectin benzoate (EB), known as an allosteric GluClα channel modulators, can downregulates AstA/AstAR expression and thereby promotes JH production.

RESULTS

Allosteric modulators (emamectin benzoate and abamectin) of the GluClα channel stimulate fecundity of female *N. lugens*

To investigate whether GluClα modulators affect fecundity in BPH, we first determined the sub-lethal and median lethal doses of emamectin benzoate (EB) on 4th instar nymphs, as well as on newly emerged males and females of BPH (Table S1). For this we employed two different bioassay methods, the rice seedling dip bioassay method and topical application bioassay method (Wu et al., 2018a; Yao et al., 2017), in order to assess both the systemic and contact toxicity of these insecticides (Table S1). We then systemically treated 4th instar nymphs of BPH, newly emerged males and females with the estimated LC_{15} or LC_{50} concentrations of EB and examined the fecundity of BPH after these individuals mated with treated or untreated individuals. We use the term “t” to represent individuals treated with EB and “ck” to indicate control individuals that were treated with insecticide diluent minus insecticide. First, we tested whether treatment of BPH with EB in the nymphal stage impairs the fecundity of BPH at the adult stage and thus exposed 4th instar BPH nymphs to the pesticide. After exposure to the LC_{15} and LC_{50} concentrations of EB, the number of eggs laid per female of BPH in ♀t × ♂t crosses increased by 1.48- and 1.40-fold compared with control ♀ck × ♂ck crosses (Figure 1A); the number of eggs laid per female of BPH in

♀t × ♂ck crosses increased by 1.53- and 2.07- fold compared with control crosses (Figure 1B); However, the number of eggs laid by per female of BPH in ♀ck × ♂t crosses did not increase significantly compared to control ♀ck × ♂ck crosses (Figure 1C).

Table S1. Determination of the toxicity of emamectin benzoate on BPH in systemic and topical application bioassays.

Treatment method	Developmental stages	Slope ± SE	LC_{15} (95%F.L.) (mg/L) or LD_{15} (95%F.L.) (pg/insect)	LC_{50} (95%F.L.) (mg/L) or LD_{50} (95%F.L.) (pg/insect)	χ^2(df)	*P value*
Systemic route	4th nymph	2.56 ± 0.487	0.87 (0.39-1.32)	2.21 (1.53-2.82)	2.68 (4)	0.61
	Adult Male	2.42 ± 0.35	0.80 (0.40-1.20)	2.13 (1.48-2.78)	2.12 (4)	0.72
	Adult Female	2.47 ± 0.41	2.33 (1.09-3.56)	6.12 (4.18-8.00)	3.56 (4)	0.50
Contact route	4th nymph	2.52 ± 0.35	15.54 (9.46-21.42)	39.90 (30.66-49.56)	2.60 (4)	0.63
	Adult Male	2.77 ± 0.57	6.72 (2.52-10.92)	15.96 (9.66-21.84)	1.23 (3)	0.75
	Adult Female	3.31 ± 0.76	18.48 (6.72-28.14)	37.80 (23.10-50.40)	0.79 (3)	0.85

Exposure of 4th instar nymphs to the LC_{15} and LC_{50} concentrations of EB in contact bioassays also significantly stimulated fecundity. After treatment with the LC_{15} and LC_{50} concentrations of EB, the number of eggs laid by per female of BPH in ♀t × ♂t crosses increased by 1.18- and 1.26-fold compared with the control (♀ck × ♂ck) (Figure 1D); The number of eggs laid per female of BPH in ♀t × ♂ck crosses increased by 1.27- and 1.56-fold compared with the control crosses (Figure 1E); However, there was no significant difference in number of eggs laid between ♀ck × ♂t crosses and controls (♀ck × ♂ck) (Figure 1F). These results reveal that EB stimulates the fecundity of females following both systemic and contact routes of exposure.

Figure 1

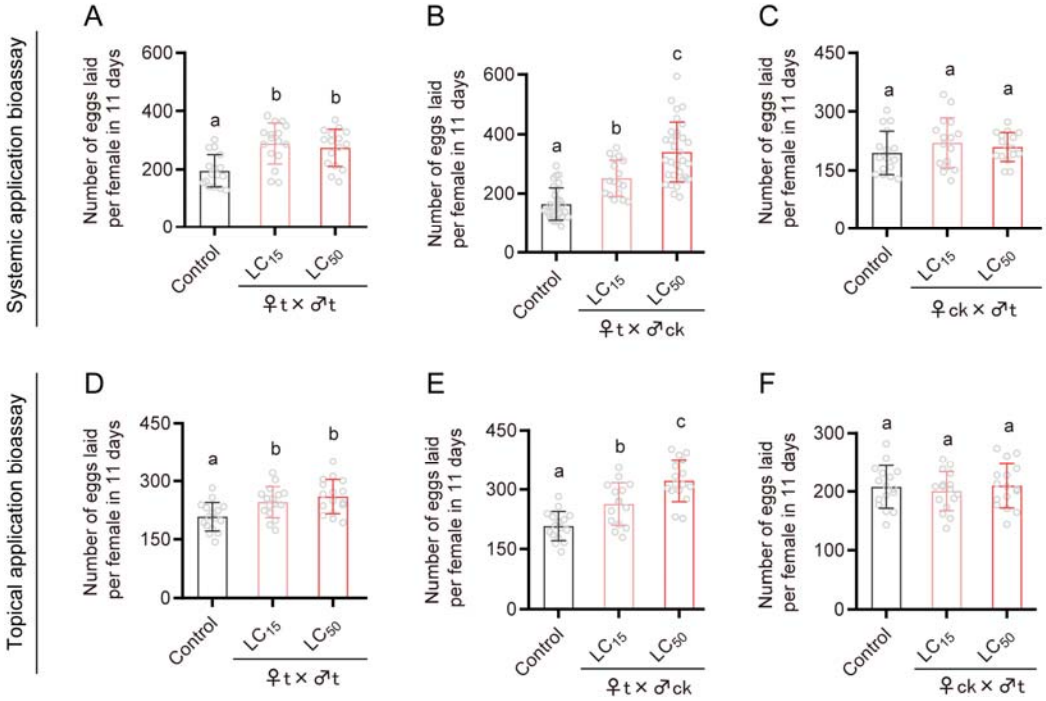

Figure 1. Fecundity of BPH following exposure to sub-lethal (LC_{15}) and median lethal (LC_{50}) concentrations of emamectin benzoate following systemic application bioassays (A: ♀t ×♂t; B: ♀t ×♂ck; C: ♀ck ×♂t) and topical application bioassays (D: ♀t ×♂t; E: ♀t ×♂ck; F: ♀ck ×♂t), respectively. The letter "t" represents treatment with insecticide, while "ck" indicates controls

that were not treated with insecticide. Insects were exposed as 4th instar nymphs. All data are presented as the mean ± s.e.m. Different lower-case letters above the bars indicate significant differences (One-way ANOVA with Tukey's Multiple Range Test, $p < 0.05$).

Next, we examined whether EB treatment of adult BPH also enhances reproduction in relation to egg laying. Indeed, treating newly emerged adults with the LD_{15} and LD_{50} concentrations of EB significantly stimulated the number of eggs laid per female (Figure 1-figure supplement 1A). Furthermore, sub-lethal exposure of 4th instar BPH nymphs to another allosteric modulator of GluClα, abamectin (LC_{15} and LC_{50} concentrations), was also found to significantly enhance oviposition (Figure 1-figure supplement 1B).

To determine whether EB administered during the fourth-instar larval stage persists as residues in the adult stage, we used HPLC-MS/MS to quantify the amount of EB present at the adult stage after exposing 4th-instar nymphs to this compound. However, we found no detectable EB residues in the adult stage following fourth-instar nymphal treatment (Figure 1-figure supplement 1C). This suggests that the mechanism underlying the increased fecundity of female adults induced by EB treatment of nymphs may differ from that caused by direct EB treatment of female adults. Combined with our previous observation that EB treatment significantly increased the body weight of adult females (Figure 1—figure supplement 3E and F), a possible explanation for this phenomenon is that EB may enhance food intake in BPH, potentially leading to elevated production of insulin-like peptides and thus increased

growth. Increased insulin signaling could potentially also stimulate juvenile hormone (JH) biosynthesis during the adult stage (Badisco et al., 2013).

Figure 1-figure supplement 1

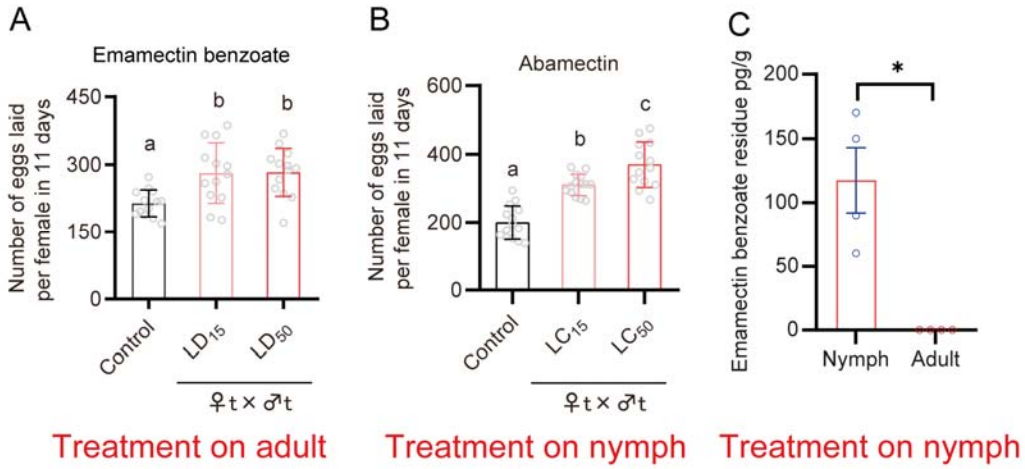

Figure 1-figure supplement 1. (A) Fecundity of BPH when newly emerged adults were treated with sub-lethal (LD_{15}) and median lethal (LD_{50}) concentrations of emamectin benzoate via topical application. (B) Fecundity of BPH when 4th instar nymphs were treated with sub-lethal (LC_{15}) and median lethal (LC_{50}) concentrations of abamectin via systemic exposure. (C) Residual levels of emamectin benzoate (EB) in brown planthoppers (BPH) following treatment. Nymphs (4th instar) were exposed to EB, and residues were quantified by HPLC-MS/MS method in nymphs (immediately post-treatment) and adults (after eclosion). No detectable EB residues were observed in adults (P=0.0037, two-tailed t-test), indicating complete metabolic clearance or degradation during development. All data are presented as the mean ± s.e.m. Different lower-case letters above the bars indicate significant differences (One-way ANOVA with Tukey's Multiple Range Test, $p < 0.05$).

To examine if EB also stimulates egg-laying in other insect species we conducted bioassays on the small brown planthopper, *Laodelphax striatellus*, the white backed planthopper, *Sogatella furcifera* and vinegar flies *Drosophila melanogaster*. In

contrast to our findings in BPH, we found that sub-lethal doses (LC_{15} and LC_{50}) of EB inhibits fecundity of female *L. striatellus*, (Figure1-figure supplement 2A-C) and has no impact on the fecundity of *S. furcifera*, (Figure1-figure supplement 2D-F). In addition, we found that sublethal doses (LC_{15}, LC_{30} or LC_{50}) of EB also inhibit fecundity in *D. melanogaster* (Figure1-figure supplement 2G and H). These results indicate that the stimulation of reproduction by EB in BPH is species-specific and does not extend to even related insect species.

Figure 1-figure supplement 2

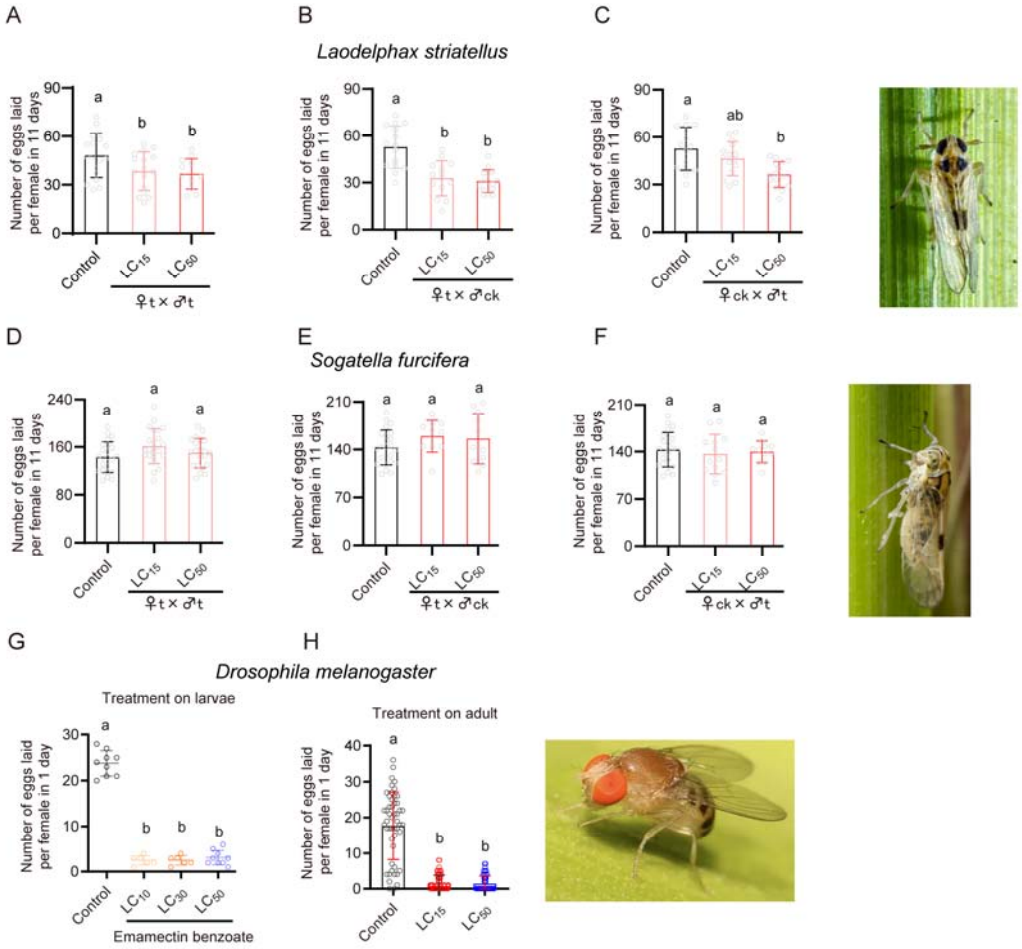

Figure 1-figure supplement 2. Fecundity of small brown planthopper, *Laodelphax striatellus*, (A-C) white backed planthopper, *Sogatella furcifera* (D-F) and vinegar fly, *Drosophila melanogaster* (G and H) when larvae and newly emerged adults were treated with sub-lethal concentrations of emamectin benzoate. All data are presented as the mean ± s.e.m. Different lower-case letters above the bars indicate significant differences (One-way ANOVA with Tukey's Multiple Range Test, $p < 0.05$).

The impact of EB treatment on BPH reproductive fitness

To better understand the effects of EB on the reproductive fitness of BPH, the duration of the preoviposition period, emergence rate, female ratio, female longevity and female weight were evaluated following exposure using systemic bioassays. The preoviposition period of females treated with the LC_{50} of EB decreased significantly compared with the control (Figure 1-figure supplement 3A). In contrast no significant effects of EB on emergence rate and female ratio were observed (Figure 1-figure supplement 3B and C). Female survival analysis showed that exposure of 4th instar nymphs to the LC_{50} of EB has no impact on female longevity (Figure 1-figure supplement 3D). Interestingly, occurrence of brachypterism (short-wing phenotype) in females and female weight were significantly increased after EB exposure (Figure 1-figure supplement 3E and F). It was reported that short-winged females usually display higher fecundity than long-winged females in BPH and two different insulin receptors determine the alternative wing morphs (Xu et al., 2015). However, whether insulin signaling is involved in the fecundity increase of BPH in our experiments requires further investigation (Ling and Raikhel, 2021; Mirth et al., 2014; Sheng et al., 2011).

233

234

Figure 1-figure supplement 3

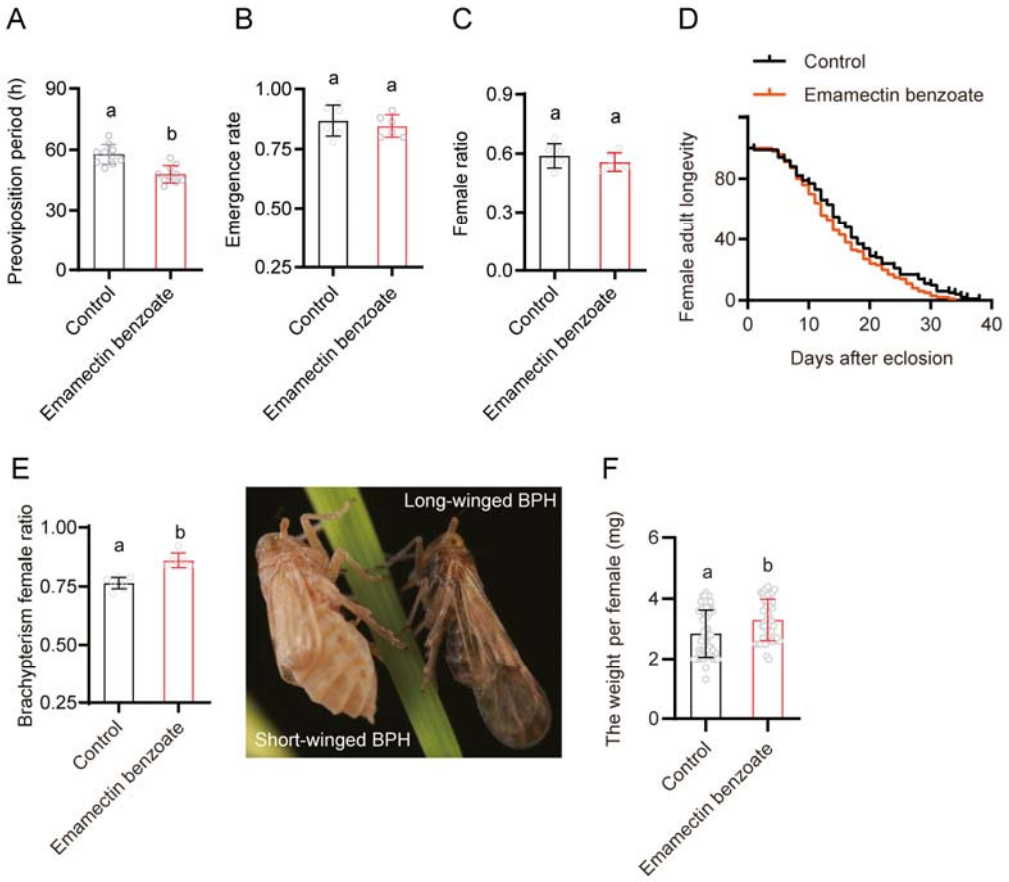

Figure 1-figure supplement 3. The impact of emamectin benzoate on the reproductive fitness of BPH. Fourth instar nymphs were treated with the LC_{50} concentration of emamectin benzoate in systemic bioassays. (A) Preoviposition period: Preoviposition refers to the period in an insect's life cycle between the time it becomes an adult and the time it starts laying eggs. (B) Emergence rate: the rate of emergence of adults; (C) Female ratio: the ratio of female (to male) insects in the total of emerged adults; (D) Female adult longevity. (E) Brachypterism female ratio: the ratio of short-winged to long-winged adults; (F) The weight per female. All data are presented as the mean ± s.e.m. Different lower-case letters above the bars indicate significant differences (Student's *t* test, $p < 0.05$).

EB promotes ovarian maturation in BPH

To investigate the cause of increased egg-laying following EB exposure, we examined whether EB influences ovarian maturation in BPH. We dissected and compared the ovaries of females treated with the LC_{50} of EB at 1, 3, 5, and 7 days after eclosion (DAE) with control females. At 3, 5, and 7 DAE, the number of eggs in the ovary of BPH in the EB treated group was significantly higher than in controls (Figure 2A and B). We furthermore observed that EB treatment of female adults also increases the number of mature eggs in the ovary (Figure 2-figure supplement 1). Hence, although EB does not affect the normal egg developmental stages (see description in next section), our results suggest that EB treatment promotes oogenesis and, as a result the insects both produce more eggs in the ovary and a larger number of eggs are laid.

Unlike the model insect *Drosophila melanogaster*, studies on oogenesis in BPH are relatively limited. Therefore, we used immunohistochemistry to stain eggs at different stages of BPH development. We captured images with a laser confocal microscope to document each stage of oogenesis in this species. We found that oogenesis in the BPH differs from that in *D. melanogaster* and belongs to the telotrophic meroistic type, where the oocyte is connected to nutrient-providing cells in the anterior trophic region of the ovariole through a nutritive cord. Oogenesis in the BPH occurs in three main compartments (Figure 2-figure supplement 2):

1. Terminal Filament (TF): This region, composed of terminal filament cells, is similar to the terminal filament structure found in Drosophila.

2. Germarium: This region is where germline stem cells (GSCs) differentiate into oocytes and follicle cells. It typically consists of cap cells adjacent to the terminal filament, germline stem cells, escort cells, and cystoblasts.

3. Egg Chamber: The egg chamber in the BPH primarily contains eggs at six developmental stages. The distinct layering of follicle cells, visible through cytoskeletal staining, is the main feature distinguishing the six different developmental stages listed in the legend of Figure 2-figure supplement 2.

We next explored whether EB treatment can enhance or impair oogenesis in BPH. However, dissection of various developmental stages revealed that EB treatment has no significant effects on developmental stages and morphology of oogenesis in BPH (Figure 2C and D). However, considering that the number of eggs laid by EB treated females was larger than in control females (Figure 1 and Figure 1-figure supplement 1), our data indicates that EB treatment of BPH can both promote both oogenesis and oviposition.

Figure 2

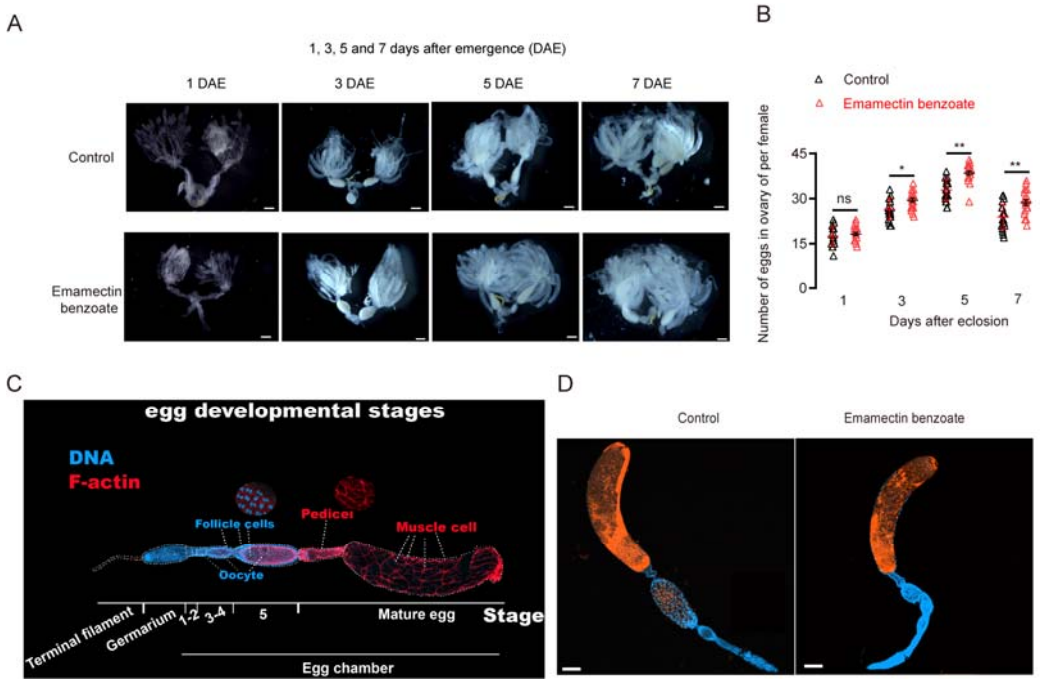

Figure 2. The impact of emamectin benzoate on ovarian maturation in BPH. Fourth instar nymphs were treated with the LC_{50} concentration of emamectin benzoate in systemic bioassays. (A) Ovarian development in EB treated BPH at 1, 3, 5 and 7 days after eclosion (DAE) compared to untreated controls. Scale bar = 1,000 µm. (B) Number of mature eggs in the ovaries of EB treated 4th instar BPH nymphs measured at 1, 3, 5 and 7 DAE compared to controls. All data are presented as the mean ± s.e.m. Asterisks indicate values significantly different from the control using student *t* test (ns, no significant; $*p < 0.05$ and $**p < 0.01$). (C) Different developmental stages of BPH eggs. (D) No impairment of emamectin benzoate on oogenesis of BPH. Scale bar = 100 µm.

Figure 2-figure supplement 1

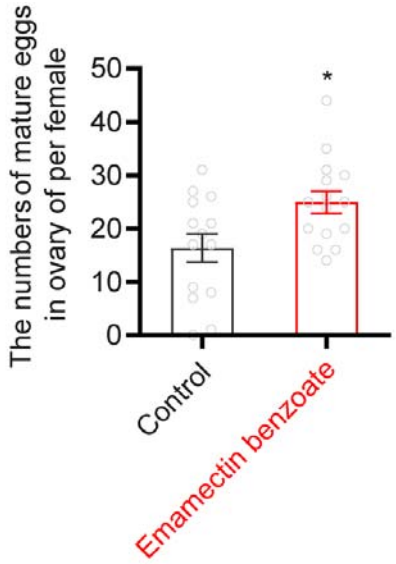

Figure 2-figure supplement 1. Number of mature eggs in the ovaries of EB treated BPH female adults compared to controls. The data are presented as the mean ± s.e.m. Asterisks indicate values significantly different from the control using student *t* test (*$p < 0.05$).

Figure 2-figure supplement 2

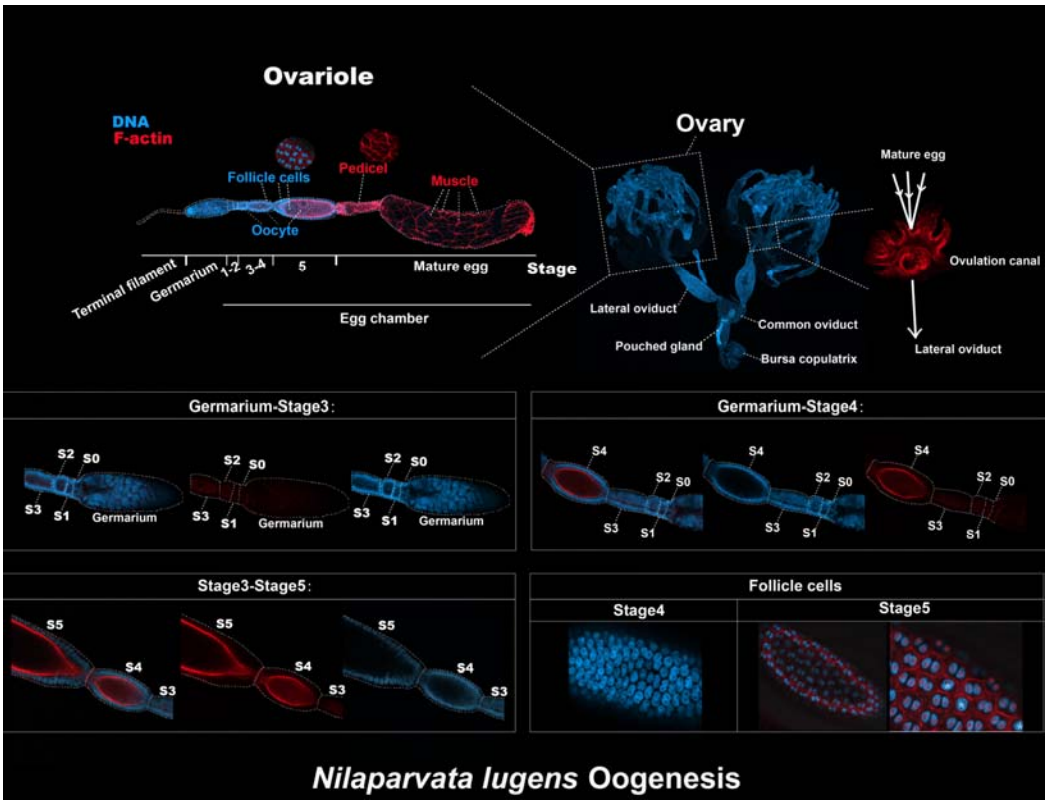

Figure 2-figure supplement 2. The oogenesis of BPH. See the main text for detailed information.

Stage 1: Connected to the germarium, the egg is trapezoidal. Stage 2: The egg is larger than in Stage 1 and is square to rectangular. Stage 3: The egg begins to elongate toward both poles, taking on an oval shape. Stage 4: The egg continues to enlarge and elongate, becoming spindle-shaped. Due to rapid growth, follicle cells on the egg surface start dividing, indicating nuclear division. Stage 5: The egg further enlarges, and most follicle cells display binucleation, the most notable feature of this stage. Small amounts of lipids start entering the egg. Stage 5 is the final stage before maturation, after which the egg enters the pedicel, a structure primarily formed by muscle fibers. The expanded mature egg stretches the muscle fibers in the pedicel, increasing the spacing between them. Stage 6: This is the mature egg

stage, which occurs after the egg passes through the pedicel. During this stage, the egg undergoes rapid growth, continuously absorbing vitellogenin and lipids (Nile red staining confirmed that Stage 6 has the highest lipid content). This absorption causes the egg's surface color to transition from the transparency seen in Stage 5 to mature eggs' dark, opaque appearance. Once the egg enters the pedicel and becomes completely opaque, it reaches full maturity. The mature egg then moves into the lateral oviduct for oviposition, completing the egg-laying process.

EB exposure increases circulating sugars and the storage of macromolecules in BPH

Nutritional status is an important indicator of reproductive fitness. Thus, to investigate whether EB affects intermediary metabolism and energy storage in BPH, glycogen, triacylglyceride (TAG) total protein content, cholesterol and four circulating carbohydrates were quantified in 4th instar BPH nymphs following exposure to the LC_{50} of EB.

We found that EB exposure has no impact on glycogen levels (Figure 2-figure supplement 2A). The amount of TAG in EB-treated BPH was 27% higher ($p < 0.05$) than those in controls, but only in BPH of the late fifth instar (5L) stage, with no significant differences observed in subsequent developmental stages (Figure 2-figure supplement 2B). The amount of total protein content in EB-treated BPH was higher than the control groups in the case of all developmental stages from 5L nymph to 7DAE (Figure 2-figure supplement 2C). EB exposure also increased cholesterol levels

at 4 and 5 DAE (Figure 2-figure supplement 2D). Compared with the solvent control, EB treatment caused significant increases ($p < 0.05$) in the levels of sucrose, glucose, fructose, and trehalose (Figure 2-figure supplement 2E-H). Thus, collectively, these data provide evidence that EB exposure leads to energy mobilization such as an increase in circulating lipids and carbohydrates in BPH.

Figure 2-figure supplement 2

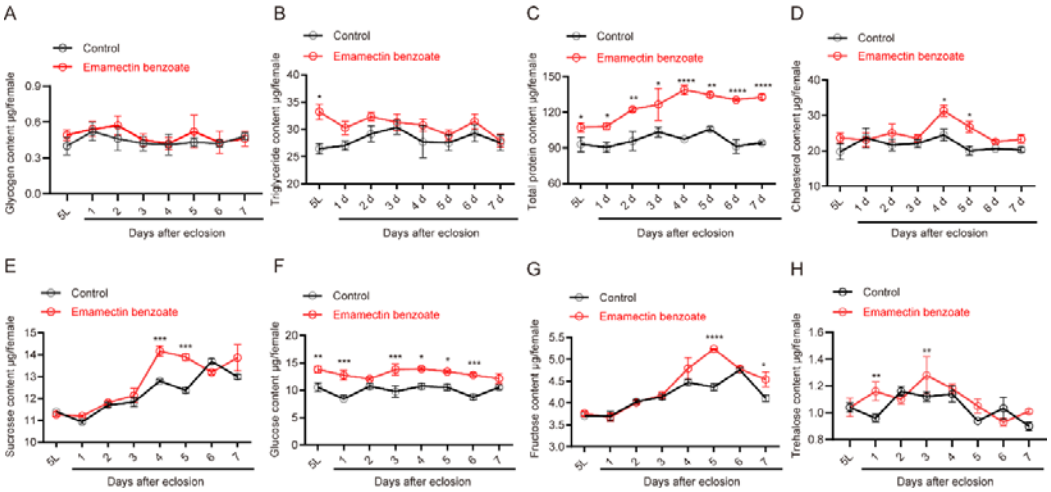

Figure 2-figure supplement 2. Amounts of Glycogen (A), TAG (B), total protein content (C), cholesterol (D) and four circulating sugars including sucrose, glucose, fructose and trehalose (E-H) after BPH exposure to EB. All data are presented as the mean ± s.e.m. The differences between the EB-treated and solvent-treated BPH were analyzed using unpaired student *t*-test (*, $p < 0.05$; **, $p < 0.01$; ***, $p < 0.001$; ****, $p < 0.0001$).

EB stimulates egg-laying that is mediated by the JH signaling pathway

Given the important role of juvenile hormone (JH) in vitellogenesis and egg development in insects (Jing et al., 2021; Ling and Raikhel, 2021; Luo et al., 2021; Santos et al., 2019; Zheng et al., 2022), we asked whether EB-treatment influences the titer of JH in BPH. As measured by ELISA, the juvenile hormone titer of BPH nymphs treated with the LC_{50} concentration of EB was significantly lower than that of controls in systemic bioassays during the middle and late stages of the 4th instar (Figure 3A). However, at 2, 3 and 4 DAE, the JH titer in the EB treated group was significantly higher than that of the control (Figure 3A). Interestingly, the titer of another important insect hormone, the steroid 20-hydroxyecdysone, was not significantly different between EB-treated

361 BPH and solvent-treated controls (Figure 3-figure supplement 1). To independently
362 validate the results of the ELISA assays, we employed HPLC-MS/MS to measure the
363 JH titer in BPH following EB exposure (Bownes and Rembold, 1987; Guo et al., 2020; Jing et
364 al., 2021). The results showed that the JH III titer significantly decreased after
365 EB-treatment at the late 4th instar nymph stage (Figure 3A and B), but significantly
366 increased at the third day after eclosion (3 DAE) (Figure 3A and C). We also
367 investigated the effects of EB treatment on the JH titer of female adults. The data
368 indicate that the JH titer was also significantly increased in the EB-treated female
369 adults compared with controls (Figure 3-figure supplement 3A). However, again the
370 steroid 20-hydroxyecdysone, was not significantly different between EB-treated BPH
371 and controls (Figure 3-figure supplement 3B).
372 To further investigate the role of JH in EB-enhanced fecundity in BPH, we treated
373 BPH with methoprene and pyriproxyfen, JH analogues or biologically active JH mimic,
374 respectively, to determine whether they can stimulate fecundity. Both compounds
375 significantly increased egg-laying in BPH (Figure 3D). Taken together, these results
376 reveal that EB exposure is associated with an increase in JH titer and that this
377 elevated JH signaling contributes to enhanced fecundity in BPH.
378 Since we found that EB could induce JH synthesis in the BPH, we asked whether
379 EB could influence the expression of genes that are involved in JH biosynthesis or
380 degradation. For this we treated 4th instar nymphs or newly emerged female adults of
381 BPH with the LC_{50} concentration of EB using systemic bioassay, and then collected
382 early (5E), middle (5M) and late (5L) stage of 5th instar nymph and 1-7 DAE female

adults for analysis. Quantitative PCR was then used to examine the expression of key genes previously implicated in the regulation of JH (Gospocic et al., 2021; Nouzova et al., 2018).

Farnesoic acid O-methyltransferase (FAMeT) (Liu et al., 2010b), is known as an important enzyme in the JH biosynthetic pathway, catalyzing methylation of farnesoic acid (FA) to methyl farnesoate (MF) (Nouzova et al., 2018). We found that this gene was significantly upregulated in 5M instar nymphs to 4 DAE following EB treatment (1.0-fold to 3.0-fold) (Figure 3E). Juvenile hormone acid methyltransferase (JHAMT) (Nouzova et al., 2018; Shinoda and Itoyama, 2003), which is involved in the biosynthesis of JH, was also upregulated in EB-treated BPH at 1 to 5 DAE compared to controls (1.5-fold to 3.0-fold) (Figure 3F). We furthermore found that EB treatment in female adults increases JHAMT expression (Figure 3-figure supplement 3C).

Methoprene-tolerant (Met), belongs to the basic helix–loop–helix Per/Arnt/Sim (bHLH-PAS) family of transcription factors and is the intracellular (nuclear) receptor of JH (Riddiford, 2020; Zhu et al., 2019). The levels of *met* mRNA slightly increased in EB-treated BPH at the 5M and 5L instar nymph and 1 to 5 DAE adult stages compared to controls (1.7-fold to 2.9-fold) (Figure 3G). However, it should be mentioned that JH action does not result in an increase of *Met*. Thus, it is possible that other factors (indirect effects), induced by EB treatment cause the increase in the mRNA expression level of *Met*.

Krüppel homolog 1 (*Kr-h1*), a transcriptional target of JH signaling, is reported to be sensitive to levels of JH and its expression levels are directly correlated with JH

405 titers (Gospocic et al., 2021; Jindra et al., 2013; Zhang et al., 2022a). We found that *Kr-h1* was
406 significantly upregulated in the adults of EB-treated BPH at the 5M, 5L nymph and 4 to
407 5 DAE stages (4.7-fold to 27.2-fold) when 4th instar nymph or female adults were
408 treated with EB (Figure 3H and Figure 3-figure supplement 3D).

409 Similarly, the expression level of *vitellogenin* (*Vg*), a key downstream component
410 of JH signaling that triggers ovarian development in insects, including BPH (Shen et al.,
411 2019), was markedly increased in females at 2–5 DAE by EB (1.7-fold to 5.5-fold)
412 (Figure 3I). During the maturation process, eggs require uptake of vg, and an increase
413 in vg content can accelerate egg maturation, producing more mature eggs. Since our
414 molecular data suggest that EB treatment leads to an upregulation of *vg* expression,
415 we propose that the increase in egg-laying caused by EB treatment is at least in part
416 due to the upregulation of *vg* (Figure 3I), which elevates Vg content, leading to
417 increased uptake of Vg by maturing eggs and resulting in the production of more
418 mature eggs.

419 Juvenile hormone esterase (JHE) is the primary JH-specific degradation enzyme
420 that plays a key role in regulating JH titers (Kamita et al., 2003). Interestingly, we
421 observed a significant upregulation of JHE mRNA levels in the early and middle 5th
422 instar nymph stage, followed by downregulation in 5L instar nymphs of EB-treated
423 BPH (1.3-fold to 2.6-fold) (Figure 3J).

424 Taken together, these results suggest that EB has a profound impact on the
425 expression of key genes involved in the biosynthesis of JH or genes in the
426 downstream signaling pathway genes that might promote egg development and

427 female fecundity. However, our data do not allow us to conclude whether the effect of
428 EB on the genes regulating the JH titer is direct or indirect.

429 To further understand whether these JH pathway-related genes are involved in
430 egg-laying behavior in BPH, we performed RNAi experiments to downregulate the
431 expression of *Kr-h1* (Figure 3-figure supplement 2A). We found that silencing of *Kr-h1*
432 diminished *vg* gene expression (Figure 3-figure supplement 2B). Importantly,
433 RNAi-induced diminishment of *JHAMT*, *Met* and *Kr-h1* genes in female BPH was also
434 found to suppress egg-laying (Figure 3K-M). However, this phenotype was rescued by
435 EB treatment, which restored egg-laying to normal levels in BPH injected with *JHAMT*,
436 *Met* and *Kr-h1* dsRNA (Figure 3K-M). Note that this rescue is possible since
437 knockdown of the genes is incomplete when using dsRNA injection (and residual
438 gene expression allows for EB action). Together these results provide a mechanistic
439 understanding of how EB enhances fecundity in BPH by modulating the expression of
440 key genes involved in JH synthesis.

441 Next, we investigated whether EB treatment could rescue the dsRNA-mediated
442 gene silencing effect. To address this, we selected the *Kr-h1* gene and analyzed its
443 expression levels after EB treatment. Our results showed that *Kr-h1* expression was
444 suppressed by ~70% at 72 h post-dsRNA injection. However, EB treatment did not
445 significantly rescue *Kr-h1* expression in gene knock down insects (*p* > 0.05) at 24h
446 post-EB treatment (Figure 3-figure supplement 4). While dsRNA-mediated *Kr-h1*
447 suppression was robust initially, its efficacy may decline during prolonged
448 experiments. This aligns with reports in BPH, where effects of RNAi gradually

diminish beyond 7 days post-injection (Liu et al., 2010a). The late-phase fecundity increase might reflect partial *Kr-h1* recovery due to RNAi degradation, allowing residual EB to weakly stimulate reproduction. In addition, the physiological impact of EB (e.g., neurotoxicity, hormonal modulation) could manifest via compensatory feedback loops or metabolic remodeling.

Figure 3

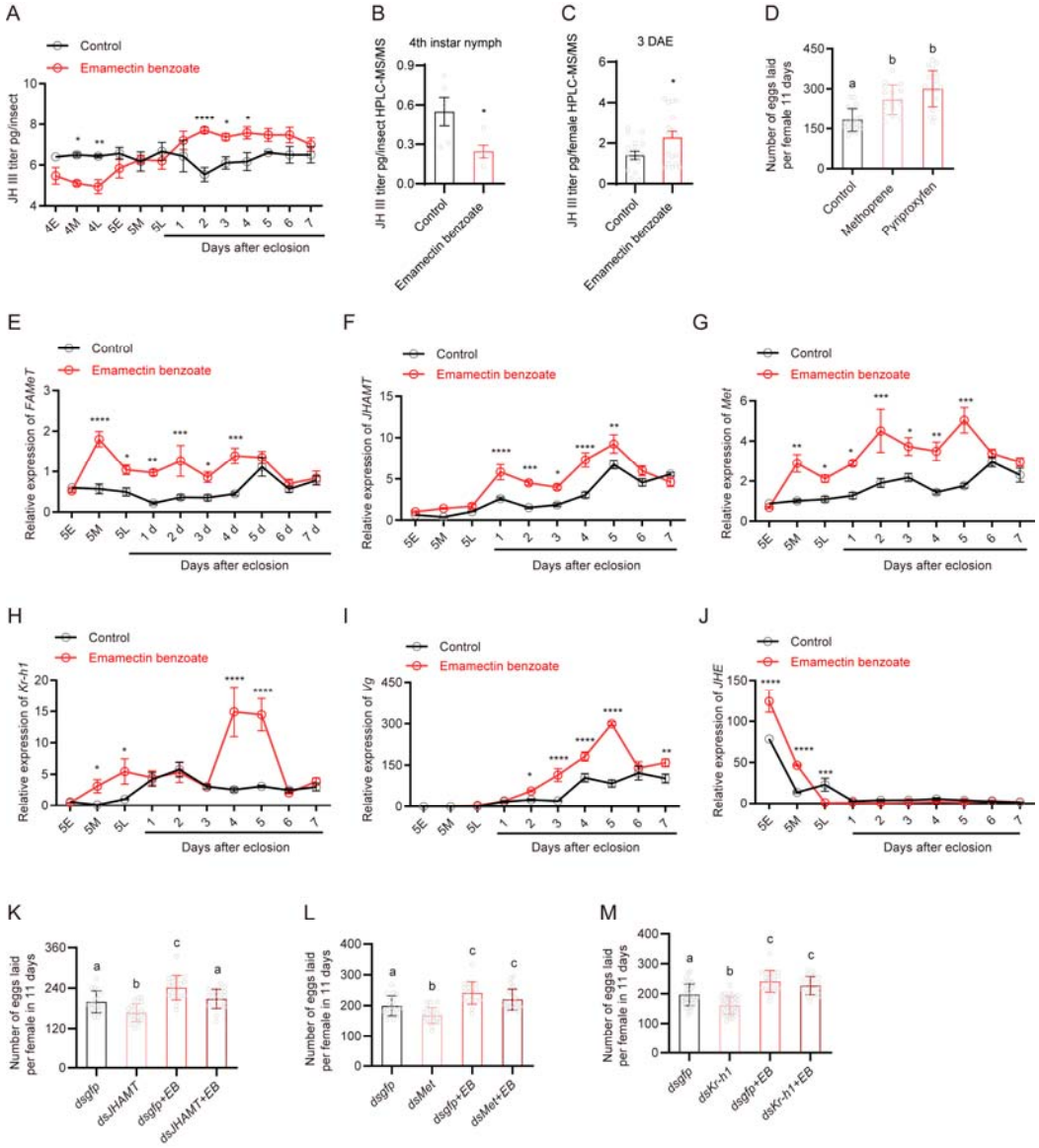

Figure 3. EB induced reproduction in BPH is mediated by components of the JH signaling pathway. (A) The titer of JH III (as measured by ELISA assay) at different developmental stages of whole body BPH when 4th instar nymphs were treated with the median lethal concentrations of EB. (B and C) The titer of JH III (as measured by HPLC-MS/MS) in whole body BPH females at 4L and 3 DAE when treated with median lethal concentrations of EB. (D) Oviposition rate of BPH when 4th instar nymphs were treated with 4 ppm methoprene or 10 ppm pyriproxyfen. (E-J) Expression of selected JH-related genes (*FAMeT*, *JHAMT*, *Met*, *Kr-h1*, *Vg*, and *JHE*) in EB-treated BPH. (K) Egg production following

silencing of *JHAMT* with or without EB application. (L) Egg production following silencing of *met* with or without EB application. (M) Egg production after silencing *Kr-h1* with or without EB application. All data are presented as means ± s.e.m. Student's *t* test was used to compare controls and treatments. One-way ANOVA with Tukey's multiple comparisons test was used to compare more than two samples. ns, no significant difference; Asterisks indicate values significantly different from the control (ns, no significant; *$p < 0.05$, **$p < 0.01$, ***$p < 0.001$ and ****$p < 0.0001$). Different lower-case letters above the bars indicate significant differences ($p < 0.05$).

Figure 3-figure supplement 1

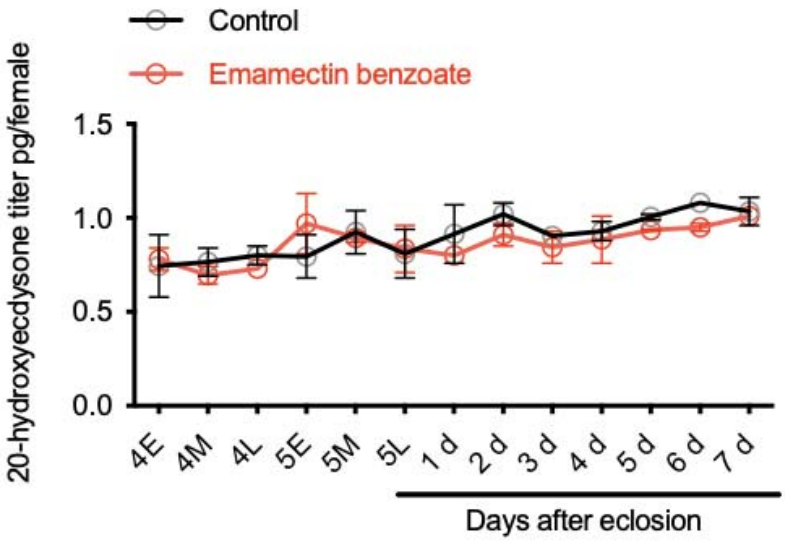

Figure 3-figure supplement 1. 20-hydroxyecdysone titer at different developmental stages of whole body BPH when 4th instar nymphs were treated with median lethal concentrations of EB.

Figure 3-figure supplement 2

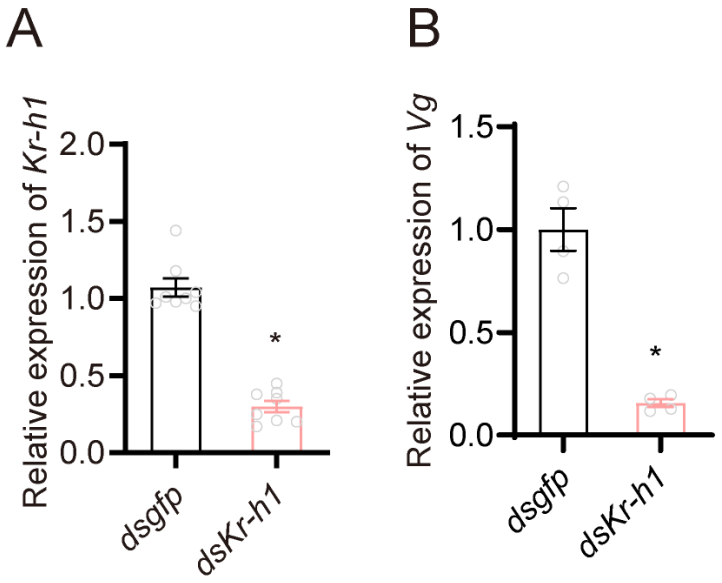

Figure 3-figure supplement 2. (A) Expression of *Kr-h1* following RNAi knockdown. (B) Expression of *Vg* when *Kr-h1* was silenced in BPH. All data are presented as means ± s.e.m. *$p < 0.05$; Mann–Whitney test.

Figure 3-figure supplement 3

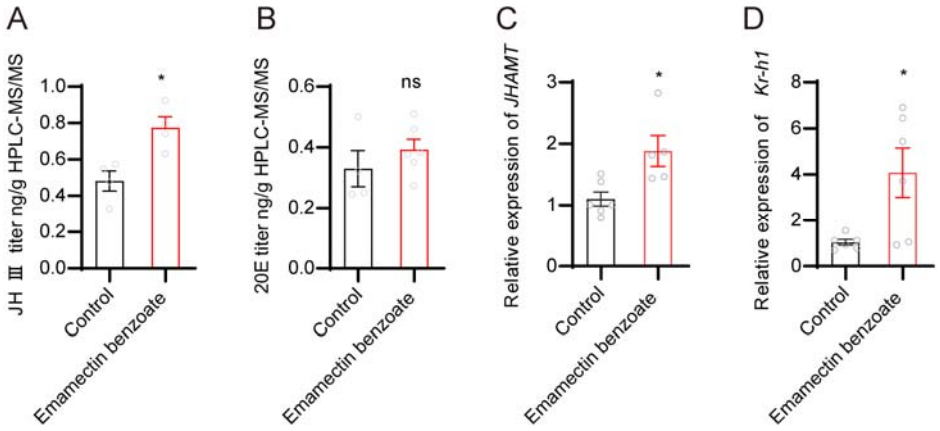

Figure 3-figure supplement 3. (A) The titer of JH III (as measured by HPLC-MS/MS) in BPH females at adult stages after treatment with median lethal concentrations of EB. (B) The titer of 20-hydroxyecdysone in BPH when female adults were treated with median lethal concentrations of EB. (C and D) Expression of *JHAMT* and *Kr-h1* in EB-treated BPH female

adults. All data are presented as means ± s.e.m. Student's *t* test was used to compare controls and treatments. Asterisks indicate values significantly different from the control (ns, no significant; *$p < 0.05$).

Figure 3-figure supplement 4

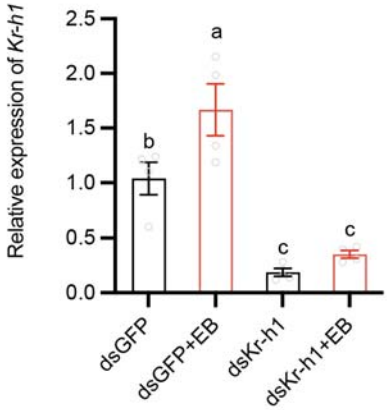

Figure 3-figure supplement 4. Evaluation of the potential of EB to reverse dsRNA-mediated silencing by quantifying *Kr-h1* gene expression. Different lower-case letters above the bars indicate significant differences (One-way ANOVA with Tukey's multiple comparisons test, $p < 0.05$).

EB induces JH biosynthesis through the peptidergic AstA/AstAR signaling pathway

In many insect species, the timing and level of JH biosynthesis can be precisely regulated by neuropeptides, such as stimulatory allatotropins (ATs) and inhibitory allatostatins (Asts), (Bellés et al., 1999; Kataoka et al., 1989; Kramer et al., 1991; Lorenz et al., 1995; Stay and Tobe, 2007; Verlinden et al., 2015; Wegener and Chen, 2022; Woodhead et al., 1989). Insects can, in a species-specific manner, produce one type of AT and three types of Asts: FGL-amide Ast (AstA) (Woodhead et al., 1989; Yin et al., 2006); myoinhibitory peptide (MIP or AstB) (Stay and Tobe, 2007) and PISCF Ast (AstC) (Wang et al., 2012). In some species, there also exists two paralogous genes of AstCs which are named *AstCC* and *AstCCC* (Veenstra, 2009, 2016). Interestingly, the allatostatic activity of these three types of Ast peptides varies between insect species so that in each species only one type of Ast (for example AstA) controls JH production (Nässel, 2002; Stay and Tobe, 2007; Wang et al., 2012; Wegener and Chen, 2022).

Analysis of neural transcriptome sequence data of BPH has revealed the presence of one AT, four types of Asts and four corresponding receptors, allatotropin receptor (A16, ATR), AstA receptor (A2, AstAR), AstB (MIP) receptor (A10, AstBR or MIPR) and AstC receptor (A1, AstCR) (Tanaka et al., 2014). We cloned the five neuropeptide genes (encoding AT, AstA, AstB/MIP, AstCC and AstCCC) and confirmed the sequences obtained from transcriptome data (Figure 4-figure supplement 1) (Tanaka et al., 2014). Interestingly, we found that AstC is missing in the genome of BPH and only AstCC and AstCCC are present (Figure 4-figure supplement 1). Next, we also cloned their corresponding receptors (Veenstra, 2009) including ATR

529 (A16), AstAR (A2), AstBR (A10) and AstCR (A1) which might be activated by AstCC
530 and/or AstCCC (Audsley et al., 2013; Veenstra, 2009; Zhang et al., 2022a). Sequence
531 alignments and phylogenetic analysis are shown in Figure 4-figure supplement 2.
532 Quantitative PCR was then used to examine whether EB treatment influences the
533 expression of the genes encoding these neuropeptides and their receptors. Treating
534 4th instar or female adult BPH with the LC_{50} concentration of EB significantly increased
535 the expression of *AT*, *ATR* and *AstCCC,* while resulting in the downregulation of *AstA,*
536 *AstB/mip, AstCC*, AstAR and *AstBR/mipr* at the adult stage (Figure 4A and B, Figure
537 4-figure supplement 3A-G). Among these, *AstA* and *AstAR* were the most
538 downregulated genes after EB treatment (Figure 4A and B, Figure 4-figure
539 supplement 3H) and thus the *AstA/AstAR* signaling system was selected for
540 subsequent functional analysis. Silencing of *AstAR* in female BPH using RNAi (Figure
541 4C), resulted in an increased number of eggs laid per female compared with
542 *dsgfp*-injected controls (Figure 4D). Interestingly, silencing *AstAR* also resulted in the
543 upregulation of *JHAMT, Met* and *Kr-h1,* which are involved in the JH
544 biosynthesis/signaling (Figure 4E-H). However, *JHE* was not influenced by AstAR
545 silencing (Figure 4I). We next investigated whether silencing the *AstAR* gene
546 influences the JH titer in BPH. Indeed, a significantly increased JH titer was observed
547 in *AstAR* silenced BPH compared with controls (Figure 4J). Thus, our data strongly
548 suggest that AstA is a key inhibitor of JH production in BPH.
549 Finally, we investigated whether injection of mature Ast and AT peptides could
550 influence the number of eggs laid and the JH titer in BPH. We synthesized one AT, six

AstAs (AstA1 to AstA6), one AstCC and one AstCCC peptide according to their determined sequences (Figure 4-figure supplement 1). Indeed, we found that injection of AstA1 and AstA6 in female adults reduced the number of eggs laid per female over 48 h (Figure 4K). We also observed that AstA1 injection decreased the JH titer as measured 16 h and 48 h after injection (Figure 4L). AT injection increased the JH titer after 2 h, but levels returned to normal 4 h after injection (Figure 4M). Collectively, our data provide compelling evidence that EB enhances reproduction in BPH probably indirectly through the AstA/AstAR and JH signaling pathways and further supports the role of AstA and AT in regulation of the JH titer in this species.

Figure 4

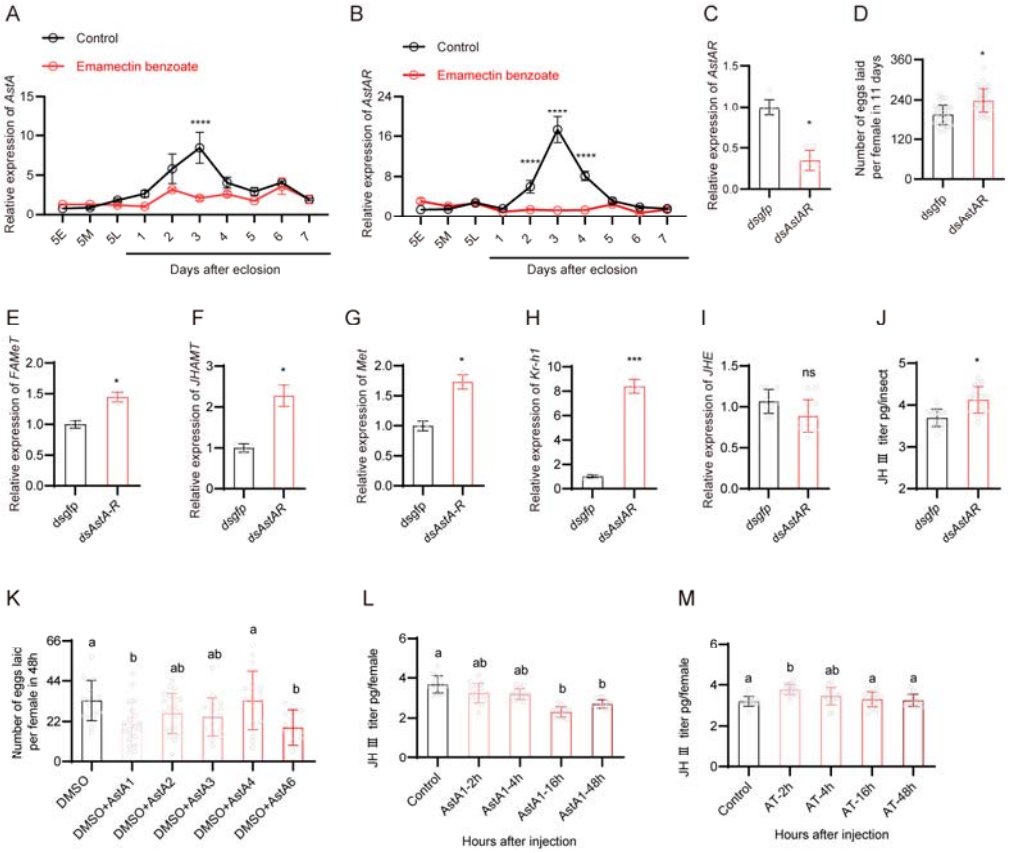

Figure 4. EB induced reproduction in BPH is mediated by the AstA/AstAR and JH signaling pathway.

(A and B) Expression of *AstA* and *AstAR* in different stages of BPH following EB treatment. (C) Downregulation of *AstAR* using RNAi leads to a reduction in mRNA expression level. (D) Egg production in female BPH following silencing of *AstAR* gene. (E-I) Expression of selected JH signaling pathway related genes (*JHAMT*, *Met*, *Kr-h1* and *JHE*) in *AstAR* silenced BPH. (J) JHIII titer of BPH females after *AstAR* gene silencing determined by HPLC-MS/MS. (K) Number of eggs laid per female in 48h following injection of the six mature AstA1-AstA6 peptides and one mature AT peptide. Fifty nanoliter of PBS (as control) and seven different peptides (20 pmol/insect) were injected into female BPH three days after eclosion. (L and M) The JH III titer of whole body BPH females at different time points following AstA or AT injection. All data are presented as means ± s.e.m. Student's *t* test was used to compare controls and

treatments. One-way ANOVA with Tukey's multiple comparisons test was used to compare more than two samples. ns, no significant difference; Asterisks indicate values significantly different from the control (ns, no significant; *$p < 0.05$, **$p < 0.01$, ***$p < 0.001$ and ****$p < 0.0001$). Different lower-case letters above the bars indicate significant differences ($p < 0.05$).

Figure 4-figure supplement 1

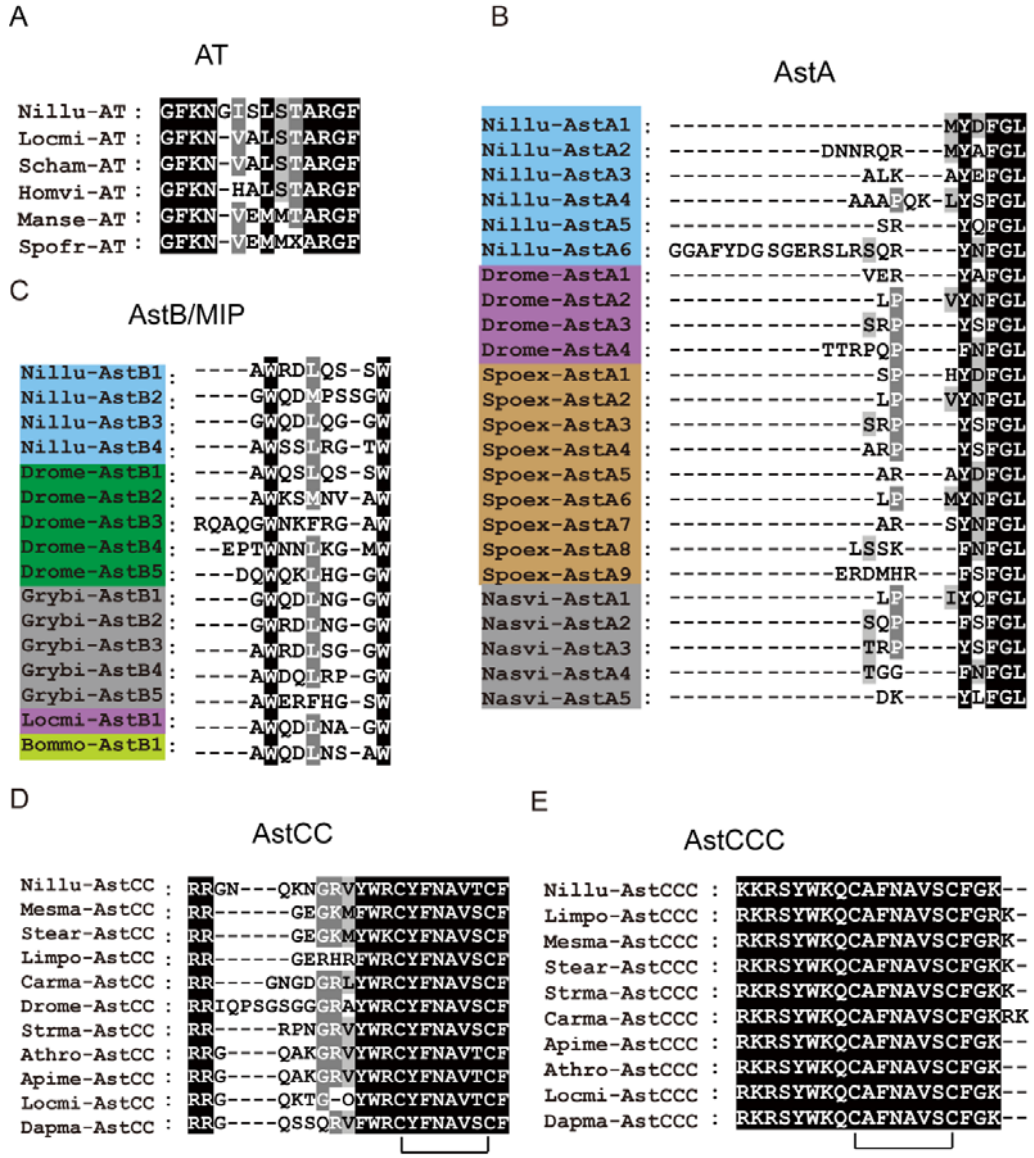

Figure 4-figure supplement 1. Alignments of the amino acid sequences of: (A) AT, (B) AstA, (C) AstB/MIP, (D) AstCC and (E) AstCCC peptides from select species. AT, AstA, AstB/MIP and AstCCC are predicted to have a C-terminal amide. The mature peptides belonging to the same species have been highlighted with the same color. Species names are as follows: Nillu (*Nilaparvata lugens*), Locmi (*Locusta migratoria*), Scham (*Schistocerca americana*), Homvi (*Homalodisca vitripennis*), Manse (*Manduca sexta*), Spofr (*Spodoptera frugiperda*), Drome (*Drosophila melanogaster*), Spoex (*Spodoptera exigua*), Nasvi (*Nasonia vitripennis*), Grybi (*Gryllus bimaculatus*), Bommi (*Bombyx mori*); Mesma (*Mesobuthus martensii*), Stear

(*Stegodyphus araneomorph*), Limpo (*Limulus polyphemus*), Carma (*Carcinus maenas*), Strma (*Strigamia maritima*), Athro (*Athalia rosae*), Apime (*Apis mellifera*), Dapma (*Daphnia magna*). Black lines under the sequences indicate the locations of the disulfide bridges in the mature peptides. The accession numbers of the sequences are listed in Figure 4-figure supplement 1 source data.

Figure 4-figure supplement 2

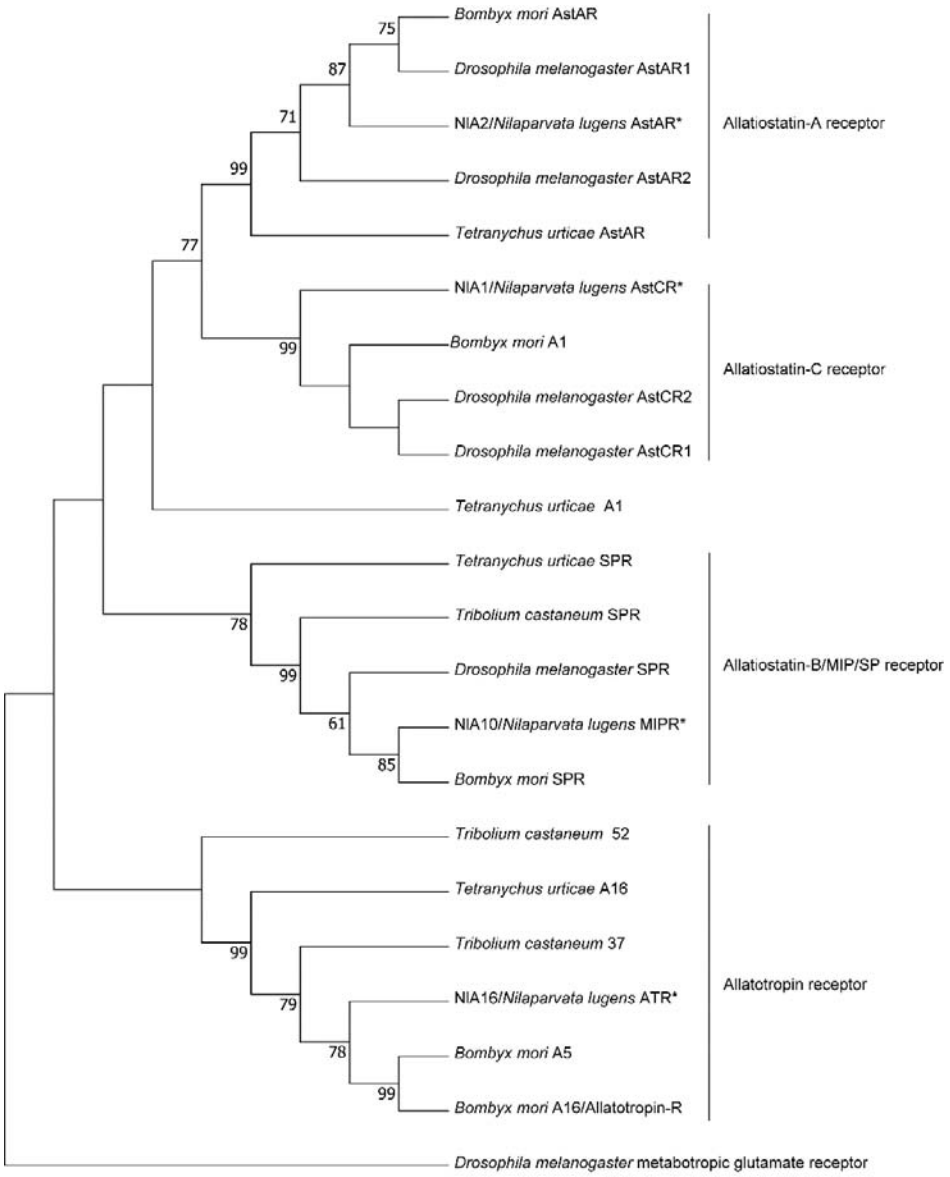

Figure 4-figure supplement 2. Phylogenetic tree of the predicted BPH (*) allatotropin receptor (A16, ATR), allatostatins A receptor (A2, AstAR), AstB (MIP) receptor (A10, AstBR or MIPR) and allatostatins C receptor (A1, AstCR) with other insect species. The tree was generated using the maximum likelihood method. *Drosophila melanogaster* metabotropic glutamate receptor was included as an outgroup. The accession numbers of the sequences used for this phylogenetic tree are listed in Figure 4-figure supplement 2 source data.

Figure 4-figure supplement 3

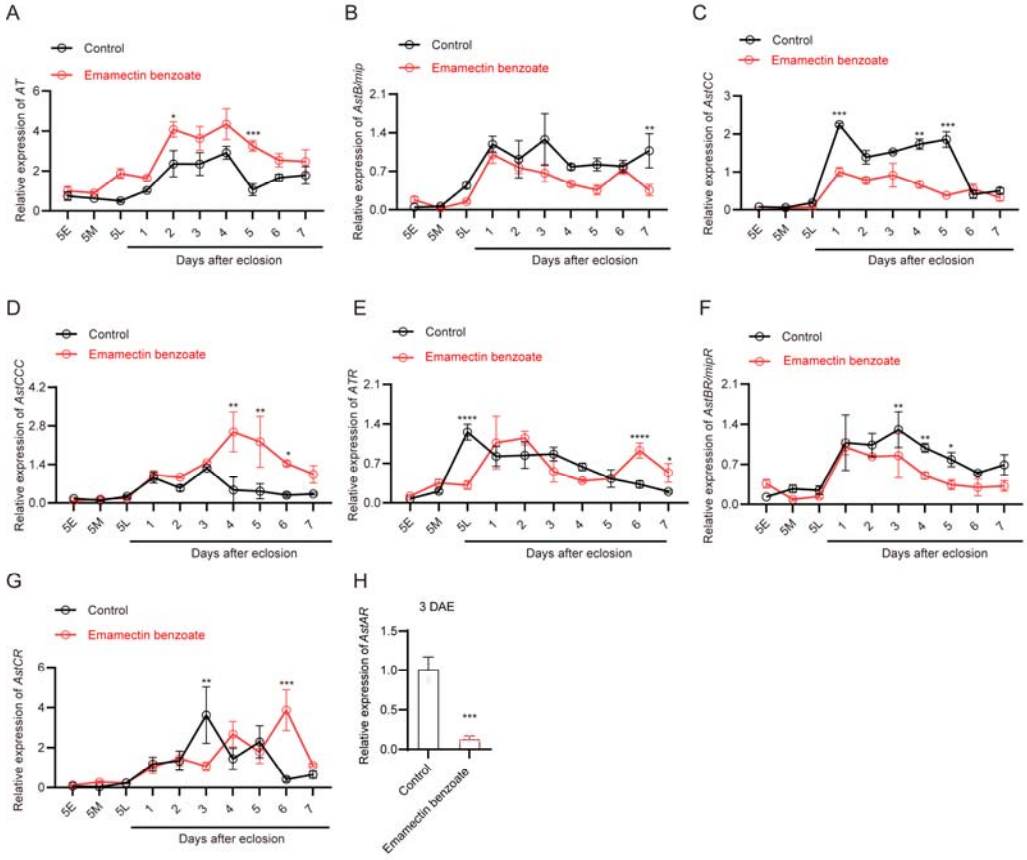

Figure 4-figure supplement 3. EB induced changes in the expression of *AT*, *AstB*, *AstCC*, *AstCCC*, *ATR*, *AstBR* and *AstCR* in BPH. All data are presented as means ± s.e.m. Student's t test was used to compare controls and treatments. ns, no significant difference; Asterisks indicate values significantly different from the control (*$p < 0.05$, **$p < 0.01$, and ***$p < 0.001$).

EB-enhanced fecundity in BPH is dependent on its molecular target protein, the GluClα channel

EB and abamectin, are allosteric modulators, which target glutamate-gated chloride channels (GluCls) (Sparks et al., 2020; Sparks et al., 2021; Wolstenholme, 2012; Wu et al., 2017). This channel is found in invertebrates only, and appears to be monomeric and formed by GluClα subunits (Wolstenholme, 2012). Hence, we examined whether EB-stimulated fecundity in BPH is mediated by its molecular target Gluclα. The full length *Gluclα* coding sequence from BPH was cloned and sequenced (Figure 5-figure supplement 1) and the impact of EB on *Gluclα* gene expression examined using quantitative PCR. Treatment of BPH with the LC_{50} concentration of EB significantly downregulated *Gluclα* gene expression at the 5E and 5M nymph stages, while upregulating *Gluclα* gene expression at 2 DAE and 5 DAE in the adult stage (Figure 5A). We also found that EB treatment in female adults also increases the *Gluclα* gene expression (Figure 5-figure supplement 3). However, we do not propose that EB is a direct transcriptional regulator of *Gluclα*, since EB and other avermectins are known to alter the channel conformation and thus their function (Wolstenholme, 2012; Wu et al., 2017). Thus, it is likely that the observed increase in *Gluclα* transcipt is a secondary effect downstream of EB signaling.

To examine the role of *Gluclα* gene in BPH fecundity, RNAi was used to knock down expression of this gene in female adult BPH (Figure 5B). A significant decrease in the number of eggs laid by per female was observed in *dsGluClα*-injected insects compared with *dsgfp*-injected insects (Figure 5C). However, treatment with EB was

found to partially rescue the decreased egg-laying phenotype induced by *dsGluClα* injection (Figure 5C). Note that this rescue is possible since knockdown of the genes is incomplete when using dsRNA injection (and residual gene expression allows for EB action). To investigate the mechanism by which *Gluclα* expression affects fecundity we examined if silencing *Gluclα* influences JH titer and JH-associated gene expression. Indeed, we observed that RNAi knockdown of *Gluclα* leads to a decrease in JH titer (Figure 5D) and down-regulation of genes including *JHAMT* which is responsible for JH synthesis, and the JH signaling downstream genes *Met and Kr-h1* (Figure 5E-G). In contrast, expression of *JHE* was not changed in the *Gluclα* knockdown insects (Figure 5H and I). We also examined whether silencing *Gluclα* impacts the *AstA*/*AstAR* signaling pathway in female adults. Knock-down of *Gluclα* in female adults was found to have no impact on the expression of *AT*, *AstA*, *AstB*, *AstCC*, *AstAR*, and *AstBR*. However, the expression of *AstCCC* and *AstCR* was significantly upregulated in *dsGluclα*-injected insects (Figure 5-figure supplement 2A-H). Further studies are required to delineate the direct or indirect mechanisms underlying this effect of *Gluclα*-knockdown.

Figure 5

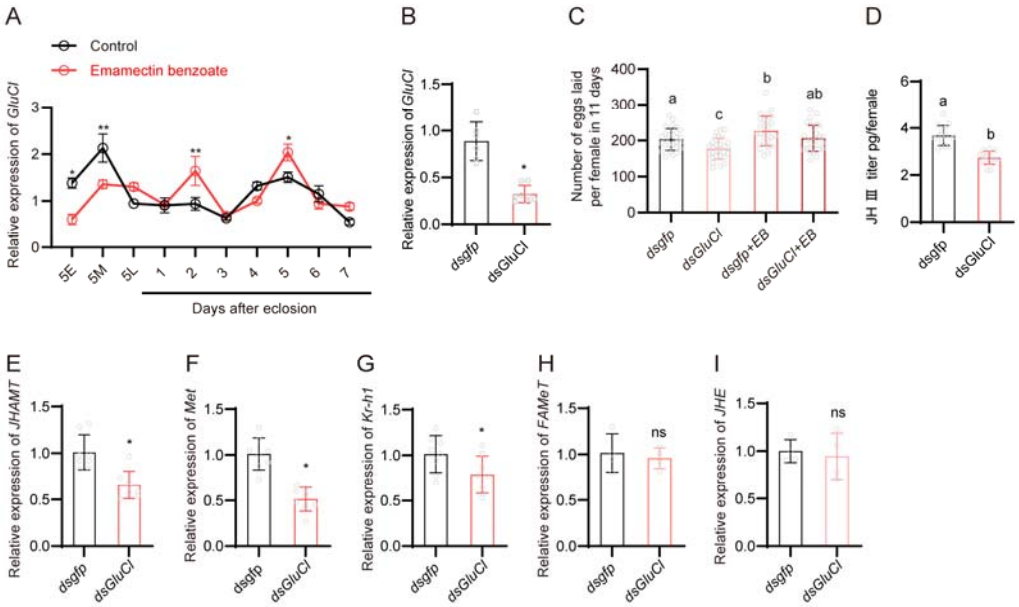

Figure 5. Role of EB and the GluCl channel in fecundity and juvenile hormone signaling in BPH

(A) Expression of *GluCl* in EB-treated and untreated BPH. (B) Expression of *GluCl* following injection of *dsGluCl* in BPH. (C) Egg production after *GluCl* gene knockdown in EB-treated and untreated BPH. (D) The JH III titer of whole body BPH females after *GluCl* gene silencing as quantified using the ELISA method. (E-I) Expression patterns of selected JH-related genes (*JHAMT*, *Met*, *Kr-h1* and *JHE*) in *GluCl* silenced BPH. All data are presented as means ± s.e.m. Student's t test was used to compare the two samples. One-way ANOVA with Tukey's multiple comparisons test was used to compare more than two samples. ns, no significant difference; Asterisks indicate values significantly different from the control (ns, no significant; *$p < 0.05$ and **$p < 0.01$). Different lower-case letters above the bars indicate significant differences ($p < 0.05$).

Figure 5-figure supplement 1

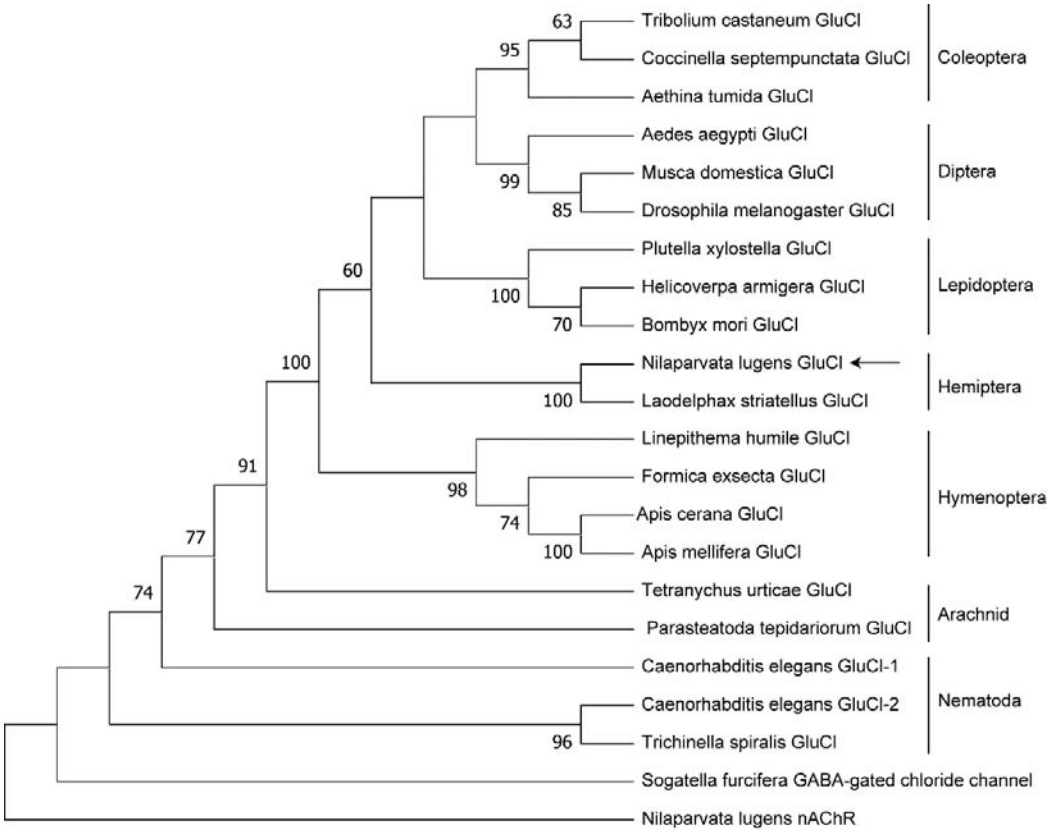

Figure 5-figure supplement 1. Phylogenetic analysis of glutamate-gated chloride channels in different species. The numbers at the nodes of the branches represent the percentage bootstrap support (1000 replications) for each branch. The *Sogatella furcifera* GABA-gated chloride channel and *Nilaparvata lugens* nAChRα6 were used as outgroup. Alignment was performed with amino acid sequences from TM1-7. The receptor names are listed in the tree. The accession numbers of the sequences used for this phylogenetic tree are listed in Figure 5-figure supplement 1 source data.

Figure 5-figure supplement 2

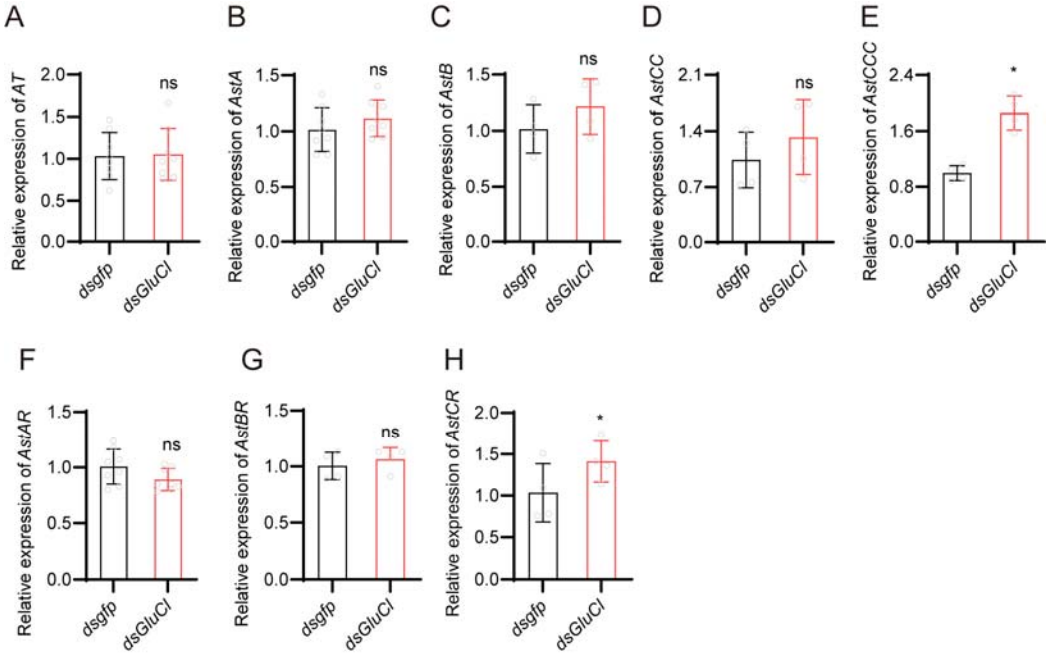

Figure 5-figure supplement 2. The expression of *AT*, *AstA*, *AstB*, *AstCC*, *AstCCC*, *AstAR*, *AstBR* and *AstCR* in BPH injected with *dsGluCl or dsgfp*. All data are presented as means ± s.e.m. Student's *t* test was used to compare the two samples. ns, no significant. Different lower-case letters above the bars indicate significant differences ($p < 0.05$).

Figure 5-figure supplement 3

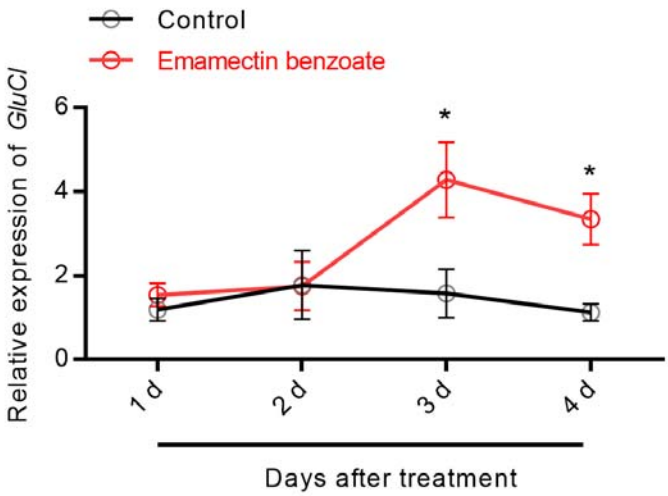

Figure 5-figure supplement 3. The expression of *GluCl* after female adult BPH were treated with EB. All data are presented as means ± s.e.m. Student's *t* test was used to compare the two samples, *, $p < 0.05$.

Discussion

Pesticide-induced resurgence of pest insects is a serious problem in rice and several other crops (Wu et al., 2020). However, the mechanisms underpinning pesticide-enhanced reproduction in insects remain poorly understood. Here we reveal that a suite of molecular actors underlie this trait that, in combination, mediate profound physiological changes in the reproductive fitness of female BPH. Our data provide fundamental insights into the molecular mechanisms by which xenobiotics modify insect reproduction and have implications for devising strategies for the control of a highly damaging crop pest. We discuss these topics below.

Sublethal doses of the GluCl modulators, EB and abamectin, stimulates fecundity in BPH

We show that in both contact and systemic assays the avermectins EB and abamectin stimulate reproduction in BPH. Thus, insecticide-enhanced reproduction is likely a key factor in the BPH resurgence observed when farmers use EB and abamectin to control leaffolders in rice crops in China (Yao et al., 2017). Although this is the first report of sublethal doses of avermectins enhancing insect fecundity, our findings are consistent with previous studies, which have shown that certain other insecticides, herbicides and fungicides stimulate BPH reproduction (Cheng et al., 2014; Ge et al., 2011; Ge et al., 2013; Wan et al., 2013; Wang et al., 2010; Wu et al., 2020; Yang et al., 2019; Zhang et al., 2014; Zhao et al., 2011). Intriguingly, we show that EB only induces fecundity in female adults and is specific to BPH, with EB exposure failing to enhance

reproduction in two related species, the small brown planthopper, *L. striatellus* and the white backed planthopper, *S. furcifera*, or the model insect *D. melanogaster*. Thus, the mechanisms underpinning this trait appear to act exclusively on female BPH and may be specific to this species. Nevertheless, our findings are of general interest since they link the molecular EB target, the GluCl channel and juvenile hormone signaling to fecundity. Furthermore, our preliminary experiments suggest that EB diminishes fecundity in *Drosophila* (see Figure 1 – Supplement 2G, H), a finding worth pursuing in this genetically tractable insect. It can be noted that the GluCl channels were first identified and cloned in the nematode worm *Caenorhabditis elegans*, where they were also found to be targets of avermectins and involved in reproduction and fecundity (Wolstenholme, 2012).

Pesticides may stimulate insect reproduction through a variety of physiological and molecular mechanisms. Our data reveal that exposure to sub-lethal concentrations of EB results in profound changes to female BPH fitness, leading to increases in female weight, contents of total protein, cholesterol, and sugars, as well as egg production and decreases in duration of the preoviposition period. Some of these findings exhibit parallels with previous studies, which demonstrated that treating third-instar BPH nymphs with either deltamethrin, triazophos, or imidacloprid led to increased soluble sugar levels in the corresponding adults (Yin et al., 2014). Such metabolites provide the energy that drives BPH reproduction and hence resurgence (Wu et al., 2020). Thus, together with prior work, our results suggest that pesticides associated with resurgence stimulate nutritional intake in BPH to fuel enhanced

energy-intensive reproduction.

The JH signaling pathway plays an essential role in EB-induced fecundity in BPH

JH is a pleiotropic hormone, which plays important roles in development and reproduction in insects (Jindra et al., 2013; Riddiford, 2008; Santos et al., 2019). Circulating JH titers are regulated by factors that control JH production in the corpora allata including biosynthetic enzymes and catabolic enzymes that regulate JH levels. Our results show that EB exposure is associated with increased circulating JH III titers in BPH females over 2–4 days after eclosion (DAE) and promotes ovarian development. Previous studies have reported that triazophos and deltamethrin treatments also lead to increased circulating JH III titers in BPH females over 1–3 days post emergence. Similarly, jinggangmycin treatments were found to lead to increased JH titers (by approximately 45–50%) in BPH females over two days post emergence (Xu et al., 2016). Thus, our findings, in combination with these previous studies, demonstrate that insecticide treatments can have dramatic effects on the regulation of key insect hormones involved in pest reproduction, which can in turn drive pesticide resurgence.

Although increased JH titers following pesticide exposure have been correlated with reduced levels of active JH esterase during the first three days PE (Ge et al., 2010), the types and numbers of mechanisms mediating the observed increase in hormone titer has remained an open question. Our data reveal that the elevated JH titer in EB-exposed BPH is associated with the upregulation a gene that encode a

753 biosynthetic enzyme for JH (*JHAMT*) and a downstream signaling gene that can
754 induce *vg* gene expression (*kr-h1*). Using RNAi we provide experimental evidence of
755 the role of these genes in the regulation of JH III and fecundity of female BPH, and
756 demonstrate that EB can restore the reduction in egg production resulting from the
757 partial RNAi knockdown of *JHAMT*, *met* and *kr-h1* expression.

758 JHMAT is an enzyme that catalyzes the conversion of inactive precursors of JH to
759 active JH in the final stages of JH biosynthesis (Nouzova et al., 2018; Shinoda and Itoyama,
760 2003). Interestingly, while it has not been previously implicated in pesticide resurgence,
761 treatment of the stored product pest *Sitotroga cerealella* with diallyl trisulfide, an
762 insecticidal compound in garlic essential oil, was found to increase JHAMT mRNA
763 levels (Shah et al., 2022). Because JHMAT is the key rate-limiting enzyme in regulation
764 of JH titer our results suggest that its enhanced expression is a key molecular
765 mechanism of pesticide resurgence in BPH.

766 Met is a ligand-activated member of the basic helix–loop–helix Per/Arnt/Sim
767 (bHLH-PAS) transcription factors and is the intracellular receptor for JH (Charles et al.,
768 2011; Jindra et al., 2015; Riddiford, 2020; Zhu et al., 2019). Kr-h1 is a zinc finger protein that
769 acts downstream of Met and is expressed in response to JH signaling. Although the
770 genes encoding these proteins have not been previously linked to pesticide
771 resurgence, our finding that they are upregulated following EB exposure, and
772 demonstration of their role of in promoting fecundity, is consistent with previous
773 studies (Santos et al., 2019). Specifically, treatment of BPH with JH III or the insecticidal
774 analogs methoprene or pyriproxifen was found to induce the expression of *Kr-h1* (Jin

et al., 2014). Furthermore, knockdown of *Met* and *Kr-h1* in brachypterous BPH females was found to result in delayed ovariole maturation and this was significantly more pronounced than the response observed in BPH treated separately with ds*NlMet* or ds*NlKr-h1* (Lin et al., 2015). This finding provides evidence of a possible interaction between *Met* and *Kr-h1* and, in combination with our data, suggests that *Met* and *Kr-h1* may act in concert to mediate EB-enhanced fecundity. However, our results showed that EB treatment can weakly increase (about 2-fold) expression of the *Met* gene in BPH (Figure 3G). Our data furthermore indicates that *Met* and *FAMeT* expression levels were not drastically influenced by EB compared with *kr-h1* and *vg* (Figure 3H and I). It should be mentioned that JH action does not directly result in the increase of *Met*. However, we cannot rule out the possibility that other factors (indirect effects), induced by EB treatment, increases the mRNA expression level of *Met*. One recent paper reported that downregulation of transcription factor *CncC* increases *met* expression in beetles (see Figure 6A in the reference) (Jiang et al., 2023). Furthermore, several studies have reported that insecticide treatment activates the *CncC* gene signaling pathway, which regulates detoxification gene expression (Amezian et al., 2023; Fu et al., 2024; Hu et al., 2021). Hence, it is possible that EB might influence the *CncC* gene pathway, which in turn induces *met* expression.

Notably, after exposing fourth-instar BPH nymphs to EB, no EB residues were detected in the subsequent adult stage. This finding indicates that the EB-induced increase in adult fecundity is initiated during the nymphal stage and s manifests in adulthood - a mechanism distinct from the direct fecundity enhancement of fecundity

observed when EB is applied to adults. We propose that sublethal EB exposure during critical nymphal stages may reprogram metabolic or endocrine pathways, potentially via insulin/JH crosstalk. For instance, increased nutrient storage (e.g., proteins, sugars; Figure 2–figure supplement 2) could enhance insulin signaling, which in turn promotes JH biosynthesis in adults (Ling and Raikhel, 2021; Mirth et al., 2014; Sheng et al., 2011). Future studies should test whether EB alters insulin-like peptide expression or signaling during development.

The EB-induced increase in fecundity in BPH is dependent on the allatostatin A signaling pathway

In addition to regulatory proteins that promote JH production, insects utilize peptides that regulate JH biosynthesis. These include the inhibitory allatostatins: FGLamides (FGLa; AstA), the W(X)6Wamides (AstB), and the PISCFs (AstC) (Nässel, 2002; Stay et al., 1996; Stay and Tobe, 2007; Tanaka et al., 2014; Wegener and Chen, 2022; Zhang et al., 2021). Interestingly, we found that EB exposure results in a marked downregulation of the expression of the genes encoding the allatostatin *AstA* and its receptor *AstAR*. We provide evidence for the functional impact of this on JH synthesis and BPH fecundity by: i) demonstrating that RNAi knockdown of *AstAR* expression results in increased JH titer and enhanced egg production, and, ii) showing that injection of female BPH with synthetic AstA peptide reduces the JH titer and decreases egg production. Thus, our data provide unequivocal evidence that AstA is a key inhibitor of JH production in BPH. This finding is consistent with previous work that has shown that FGLa/ASTs (AstA) inhibit JH biosynthesis in cockroaches, and

termites (Woodhead et al., 1989; Yagi et al., 2005). To our knowledge, our study is the first report of insecticides down-regulating the expression of the neuropeptide receptor, *AstAR*, and linking this to increases in JH titer and enhanced reproduction in insects.

Interestingly knockdown of the *AstAR* resulted in significant increases in the expression of genes involved in JH biosynthesis/signaling including *JHAMT*, *Met* and *Kr-h1*. Related to this finding, previous work has shown that knockdown of the AstA receptor gene, *Dar-2*, in *D. melanogaster* results in changes in the expression of genes encoding *Drosophila* insulin-like peptides (DILPs) and adipokinetic hormone (AKH) (Hentze et al., 2015). Together with our findings, this demonstrates that AstA receptors may modulate the expression of numerous downstream genes involved in metabolism, energy storage and reproduction. In the case of pesticide resurgence our findings suggest that EB may act directly and/or indirectly on several genes that affect JH signaling and fecundity.

The GluCl **plays a role in EB-induced fecundity in BPH**

EB and abamectin are allosteric modulators of GluCls (Sparks et al., 2020; Sparks et al., 2021; Wu et al., 2017). Our data revealed that EB exposure increases the expression of the GluCl in the adult stage of BPH, and knockdown of GluCl expression resulted in a reduction in both JH levels and egg production and egg laying. This EB action on *GluClα* expression is likely indirect, and we do not consider EB as transcriptional regulator of *GluClα*. Thus, the mechanism behind EB-mediated induction of *GluCl*α remains to be determined. It is possible that prolonged EB exposure triggers feedback

841 mechanisms (e.g. cellular stress responses) to counteract EB-induced *GluCl*α
842 dysfunction, leading to transcriptional upregulation of the channel. Hence, considering
843 that EB exposure in our experiments lasts several days, these findings might
844 represent indirect (or secondary) effects caused by other factors downstream of GluCl
845 signaling that affect channel expression.

846 There are several studies showing that insects treated with insecticides display
847 increases in the expression of target genes. For example, the relative expression level
848 of the ryanodine receptor gene of the rice stem borer, *Chilo suppressalis* was
849 increased 10-fold after treatment with chlorantraniliprole, an insecticide which targets
850 the ryanodine receptor (Peng et al., 2017). In *Drosophila*, starvation (and low insulin)
851 elevates the transcription level of the receptors of the neuropeptides short
852 neuropeptide F and tachykinin (Ko et al., 2015; Root et al., 2011). In BPH, reduction in
853 mRNA and protein expression of a nicotinic acetylcholine receptor α8 subunit is
854 associated with resistance to imidacloprid (Zhang et al., 2015). Knockdown of the α8
855 gene by RNA interference decreased the sensitivity of *N. lugens* to imidacloprid (Zhang
856 et al., 2015). Hence, the expression of receptor genes may be regulated by diverse
857 factors, including insecticide exposure.

858 Interestingly, the GluCl has been reported to inhibit the biosynthesis of JH in the
859 cockroach, *Diploptera punctata* (Liu et al., 2005). Recent work has also shown that
860 modulation of glutamatergic signals may contribute to the photoperiodic control of
861 reproduction in bean bug, *Riptortus pedestris* (Hasebe and Shiga, 2022). Furthermore,
862 work on *D. punctata* has revealed that application of the GluCl channel agonist

ivermectin, which like EB belongs to the avermectin family, caused a decline in JH synthesis in the corpus allatum (Liu et al., 2005). While the inhibitory effect of ivermectin observed in this previous study differs from the activating effect of EB we observed in our study, it implicates a role for the GluCl channel in the regulation of JH regulation.

Conclusion

Our study has revealed that exposure of BPH to EB affects a diverse suite of genes that act in combination to enhance the JH titer and thus increase female fecundity. A schematic of how these factors promote ovarian maturation in the adult stage of *N. lugens* through the AstA and JH signaling pathway is provided in Figure 6. Our findings provide the foundation for further work to understand how these genes interact and the mechanisms by which their expression is activated or repressed by EB. Furthermore, our findings provide fundamental insights into the molecular response in insects to xenobiotic stress and illustrate that pesticides can have unexpected and positive impacts on pest populations. In this regard our findings also have applied implications for the control of a highly damaging crop pest. Previous studies have reported that avermectins such as abamectin are toxic to the wolf spider *Pardosa pseudoannulata*, which is the main predator of BPH in rice crops (Chen et al., 2017; Sogawa, 2015). Thus, these insecticides both stimulate reproduction in BPH and kill their natural enemies providing a ‘perfect storm’ for inducing damaging BPH outbreaks. Based on these findings, to avoid BPH resurgence, we suggest that the agents, EB and abamectin, should not be (or rarely be) applied to rice plants at growth

stages when BPH are present. On a more optimistic note, our findings have identified numerous genes that play key roles in BPH reproduction and thus represent promising targets for the development of novel controls against this important pest.

Figure 6

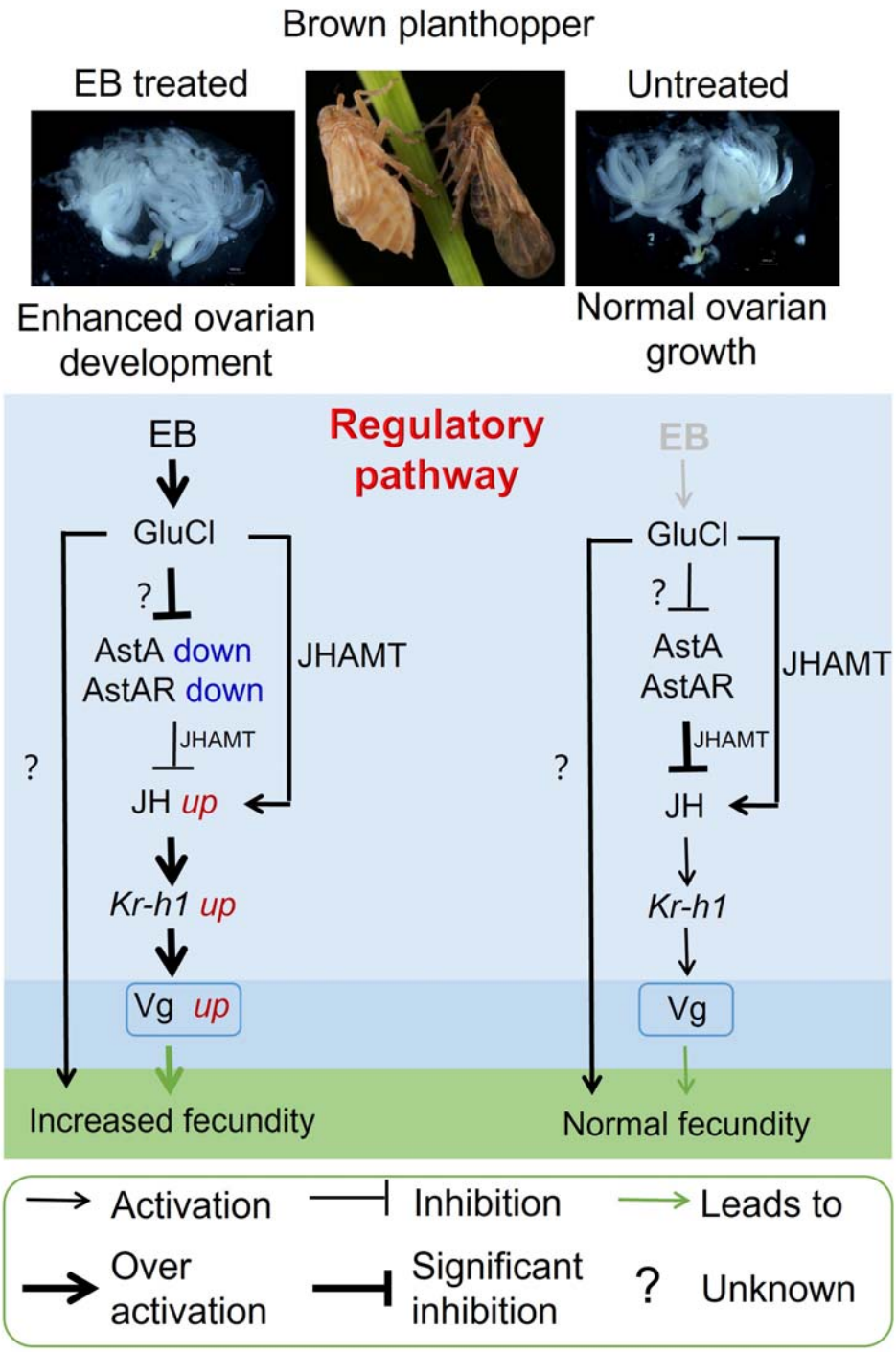

Figure 6. Schematic of the proposed regulatory pathway of EB-enhanced fecundity in BPH. Emamectin benzoate (EB) exposure results in the upregulation of genes that promote

JH signaling pathway (*JHAMT and Kr-h1*) and the downregulation of genes that inhibit it (allatostatin, Ast*A* and allatostatin A receptor, *AstAR*). This transcriptome reprograming is dependent on the allosteric action of EB on its molecular target the glutamate-gated chloride channel (GluCl) receptor. Note that the mechanism of action on the GluCl is unknown in BPH, but likely the channel conformation changes and renders the receptor dysfunctional. Importantly, we do not suggest that the GluCl upregulation is due to direct action of EB on the channel. The resulting increased JH titer promotes vitellogenin (vg) biosynthesis and increased fecundity in EB exposed insects. We observe significant cross-talk in the expression of genes that inhibit JH production and those that promote it, with *AstAR* inhibiting the expression of *JHAMT, Met* and *Kr-h1* and *GluCl* activating the expression of *JHAMT* which is responsible for JH synthesis, and the JH signalling downstream genes *Met and Kr-h1*.

Materials and methods

Insects

BPH was initially collected from Wanan, JiangXi Province in 2020, reared on 'Taichung Native 1' (TN1) rice seedlings in the laboratory without exposure to any insecticides. The strain was maintained in a climatic chamber at 27 ± 1°C, with relative humidity of 70 ± 10% and a light: dark = 16 h: 8 h photoperiod.

Chemicals

Emamectin benzoate (95.2%) was obtained from Hebei Weiyuan Co., Ltd. (Hebei, China). Abamectin (96.8%) was obtained from Hebei Weiyuan Co., Ltd. (Hebei, China). Pyriproxyfen (98%) was obtained from Shanghai Shengnong Co., Ltd. (Shanghai, China). Methoprene (S)-(+) (mx7457-100mg) was purchased from Shanghai MaoKang Biotechnology Co., Ltd., (Shanghai, China). Juvenile hormone standard sample (J912305-10mg) was purchased from Shanghai Macklin

Biotechnology Co., Ltd., (Shanghai, China).

Bioassay

Different life stages of insects were used to perform bioassays to investigate the effects of insecticide on nymphs and adults. To test whether treatment of the nymph stage of insects would promote reproduction in female, we used 4th instar nymphs of BPH or 3rd instar nymph of *Laodelphax striatellus* and *Sogatella furcifera* to perform bioassays. To test whether treatment of the adult stage of insects would promote reproduction in female, we used newly emerged male and female BPH.

Systemic bioassays: The rice-seeding dipping bioassay method was used to evaluate the susceptibility of BPH, *L. striatellus* and *S. furcifera* to EB. Technical-grade insecticides were dissolved in acetone as stock solution then diluted in a series of six concentrations with water containing 0.1% Triton. Selected rice seedlings at the 6-8 cm growth stage were dipped in insecticide solutions for 30 s and then air-dried at room temperature. The roots of the rice seedlings were wrapped with cotton strips and seedlings placed in a plastic cup 5 cm in diameter. Fifteen insects were introduced into each plastic cup for each replicate. The top of the cup was then sealed with gauze to prevent escape. All experiments comprised at least three biological replicates. Control rice seedings were treated with 0.1% Triton X-100 water solution only. All treatments were maintained under standard conditions of 27 ± 1 °C and 70–80% relative humidity with a 16 h light/8 h dark photoperiod. Mortality was assessed after 4 d for *N. lugens* or 2 d for *L. striatellus* and *S. furcifera* after treatment with insecticides. The insects were considered dead if they were unable to move in

response to gentle prodding with a fine brush.

For *Drosophila* larval bioassays, we adopted a method described previously in our lab with minor modifications (Huang et al., 2020). Briefly, twenty third instar larvae were placed in fly vials containing fly food (based on corn powder, brown sugar, yeast and agar) supplemented with EB of different concentrations. Four concentrations (LC_{10}, LC_{30} and LC_{50}) were tested together with a negative (no insecticide) control. For *Drosophila* adult bioassays, we selected virgin females three days after eclosion. Several concentrations were overlaid onto fly food in standard *Drosophila* vials and allowed to dry overnight at room temperature. A total of 15 adult flies (three days after eclosion) were then added to each vial and mortality assessed after 2 d. Four replicates were carried out for each concentration. Control mortality was assessed using vials containing food with solvent minus insecticide.

Contact bioassays: For topical bioassays working insecticide solutions were prepared in acetone. 4th instar nymphs or newly emerged males/females were anesthetized with carbon dioxide for 5 s, and then 0.04 μl/insect test solution applied topically to the dorsal plates with a capillary micro-applicator (Yao et al., 2017). Insects were then placed in an artificial climate incubator with a temperature of 27±1°C, a photoperiod of 16:8 h (L:D), and a humidity of 70%±10%. Mortality was determined 2 d after treatment. Data with over 20% mortality in the control treatment were discarded, and the assay was repeated at least three times.

Fecundity assays

Fourth instar nymphs of BPH and 3rd instar nymph of *L. striatellus* and *S. furcifera*

were treated with the LC_{15} and LC_{50} of EB, and then transferred to fresh rice seedlings. After eclosion, the adults were used in the following experiment. Newly emerged treated adults and untreated adults were paired to produce four groups: untreated males and untreated females (♂ck×♀ck; ck indicates untreated); untreated males and treated females (♂ck×♀t; t indicates insecticide treated); treated males and untreated females (♂t×♀ck); treated males and treated females (♂t×♀t). Each group comprised at least 10 mating pairs. All pairs were transferred to glass cylinders (diameter 5 cm and height 20 cm) containing rice plants (25 days old almost 20 cm high) as a food source for eleven days. The number of eggs and nymphs in plants were counted under a microscope.

For *Drosophila* egg-laying assays, we adopted our previous method (Wu et al., 2019). Briefly, insecticide-treated virgin females were paired with untreated males for three days and then the mated females transferred into the *Drosophila* ovipositing apparatus. The number of eggs were counted after 16 hours.

Fitness analysis

The fitness of EB-treated BPH were analyzed using methods reported previously (Zeng et al., 2023). We selected two groups, (♂ck×♀ck) and (♂ck×♀t), to study the effects of the LC_{50} concentration of EB on BPH fitness. In the case of systemic exposure, 4th instar nymphs of BPH were treated with the LC_{50} of EB for 4 days and then transferred to tubes containing untreated rice plants for individual rearing. The rice plants were replaced every three days with untreated plants. The emergence ratio, female ratio, preoviposition period, female longevity, brachypterism female ratio and

female weight were calculated.

Examination of ovarian development

Adult females from ♂ck×♀ck control and ♂ck×♀t group on 1, 3, 5, 7 DAE were dissected to observe ovarian development. The mature eggs in the ovary were photographed and recorded. Each group comprised at least fifteen replicates.

To examination whether EB treatment impairs egg maturation, we dissected untreated or EB-treated ovaries and fixed them in 4% paraformaldehyde (PFA) in phosphate buffered saline (PBS) for 30 min at room temperature. After four washes of 10 min (4 × 10 min) in PAT3 (PBS with 0.5% Triton X-100 and 0.5% bovine serum albumin), the ovaries were then incubated with DAPI (4',6-diamidino-2-phenylindole, 100 nM) and Actin-stain 670 Fluorescent Phalloidin (200 nM). Imaging was performed using a Zeiss LSM980 confocal laser microscope.

Measurements of glycogen, triglyceride, total protein content, cholesterol and four sugars

The content of glycogen, triglyceride, cholesterol and total protein was determined by spectrophotometry at 620 nm, 510 nm, 510 nm and 562 nm respectively using the glycogen assay kit (A043-1-1), triglyceride reagent kit (A110-1-1), cholesterol assay kit (A111-1-1) and total protein assay kit (A045-2-2) obtained from Nanjing Jiancheng Bioengineering Institute following the manufacturer's instructions. The determined results were normalized to the protein content in the sample, which was determined using BCA Protein Assay Reagent Kit

(Thermo Scientific, Waltham, USA). Each sample contained tissue extracts from five adult female BPH, with three biological replicates per sample.

To assess the content of four sugars (sucrose, glucose, fructose and trehalose) in the extract of BPH tissue, the same extraction method was used as above. Sugar content was quantified using the colorimetric method by scanning at 290 nm, 505 nm, 285 nm and 620 nm respectively using the sucrose reagent kit (A099-1-1), glucose reagent kit (F006-1-1), fructose reagent kit (A085-1-1) and trehalose reagent kit (A150-1-1) obtained from Nanjing Jiancheng Bioengineering Institute based on the manufacturer's instructions. Each sample contained tissue extracts from five adult female *N. lugens*, with three biological replicates per sample.

Determination of Juvenile hormone III and 20-hydroxyecdysone titers of BPH by ELISA

The titer of Juvenile hormone III in BPH was measured using the Juvenile hormone ELISA Kit (Lot Number: HLE92086, Shanghai HaLing Biotechnology Co., Ltd., Shanghai, China) which employs the dual-antibody sandwich ELISA method. The titer of 20-hydroxyecdysone in BPH was measured using the 20-hydroxyecdysone ELISA Kit (Lot Number: ZK14705, Shanghai ZhenKe Biotechnology Co., Ltd., Shanghai, China). At least three biological replicates were employed for each treatment.

Determination of Juvenile hormone III titer in BPH using HPLC-MS/MS

The whole bodies of 5 individual BPH were mixed with 1 ml of n-hexane, followed

by centrifugation at 10,000×g for 10 min, the upper hexane layer was then dried with nitrogen, dissolved in methanol and sonicated for 10 min, after centrifugation at 10000×g for 10 min, the supernatant was collected through the organic filter membrane of 0.22 μm into 2 ml vials for JH □ determination. JH □ standard sample (J912305-10 mg) purchased from (Shanghai McLean Biochemical Technology Co. Ltd), dissolved in methyl alcohol as stock solution 10,000 mg/L was diluted in a series of six concentration gradients to serve as a reference. Liquid chromatography-tandem mass spectrometry (LC-MS/MS) was then carried out using UPLC Xevo TQ-S Micro (Waters technology), quantitative method according to the external standard, the chromatographic column was EC-C18 (4.6 mm×150 mm, 2.7 μm), column temperature was 30°C，injection volume was 20 μl, elution flow rate was 0.3 ml/min, and the mobile phase was acetonitrile:formic acid water (90:10), detection wavelength was 218 nm, the peak height was used for quantification.

Determination of EB content using HPLC-MS/MS

4L BPH were systemically treated with EB as outlines above, samples were collected at 3 days post-treatment and transferred to healthy rice seedlings for 3 more days, after which another sample was collected. Each experiment included 3 biological replicates, with approximately 20 brown planthoppers weighed per replicate. The weight of each sample was recorded, and 400 μL of methanol was added to each sample. The samples were then ground for 180 seconds at 65 Hz, followed by ultrasonic treatment at 4°C for 30 minutes. Next, 400 μL of n-hexane was added, and

the mixture was vortexed to mix thoroughly. The samples were centrifuged at 12,000 rpm for 15 minutes at 4°C, and the supernatant was collected into a centrifuge tube and evaporated to dryness in a concentration evaporator. Then, 200 μL of methanol was added for reconstitution, followed by vortex mixing. The samples were centrifuged again at 12,000 rpm for 15 minutes at 4°C, and the supernatant was analyzed using the LC-MS/MS system. The EB standard was purchased from Shanghai Minxin Biotechnolog. Six concentration gradients were used for elution. The column temperature was maintained at 40°C, and the flow rate was set to 0.300 mL/min. Liquid chromatography-tandem mass spectrometry (LC-MS/MS) was performed using a Waters Acquity UPLC system and an AB SCIEX 5500 QQQ-MS mass spectrometer. The chromatographic column used was Acquity UPLC BEH C18 (1.7 μm, 2.1 mm × 100 mm). A standard curve was generated for content calculation.

Cloning, sequence and phylogenetic analysis

The NCBI database and BLAST program were used to carry out sequence alignment and analysis. Open Reading Frames (ORFs) were predicted with EditSeq. Primers were designed using the primer design tool in NCBI. Total RNA Extraction was extracted from 30 adults BPH using TRIzol reagent (Invitrogen, Carlsbad, CA, USA) according to the manufacturer's instructions. cDNA was synthesized using the Biotech M-MLV reverse transcription kit. Full-length gene sequences were amplified by PCR using cDNA as template and Rapid Taq Master Mix (Vazyme Biotech, Cat# P222-02). The PCR product was purified on a 1% agarose gel, cloned into pClone007

Simple Vector Kit (Tsingke Biotech, Cat# TSV-007S), and then sequenced using the 3730 XL DNA analyzer (Applied Biosystems, Carlsbad, CA, USA). Table S2 contains a list of the primers used in this study.

The exon and intron architectures of *AT*, *AstA*, *AstB*, *AstCC* and *AstACCC* were predicted based on the alignments of putative ORFs against their corresponding genomic sequences. Sequence similarity/annotations and orthologous gene searches were performed using BLAST programs available in NCBI. Multiple alignments of the complete amino acid sequences were performed with Clustal Omega (http://www.ebi.ac.uk/Tools/msa/clustalo). Phylogeny was conducted using the maximum likelihood technique to create phylogenetic trees and these were bootstrapped with 1000 replications were used using the MEGA 6 software (Tamura et al., 2013).

RNA interference

Double-stranded RNA (dsRNA) of *gfp* (green fluorescent protein), *JHAMT* (juvenile hormone acid O-methyltransferase,), *Met* (methoprene-tolerant), *Kr-h1* (krüppel homolog 1), *AstAR* (allatostatin-A receptor) and *GluCl* (glutamate-gated chloride channel) was prepared using Ambion's MEGAscript T7 kit following the manufacturer's instructions. The primer sequences for double-stranded RNA synthesis are listed in Table S2. Newly emerged females were injected with 40 nl (5,000 ng/μl) of double-stranded RNA of *gfp* (*dsgfp*) or double-stranded RNA of the target genes in the conjunctive part between prothorax and mesothorax of insects. In the RNAi experiments, BPH were then treated with the LC_{50} of EB 24h after dsRNA

injection and the whole body sampled for qRT-PCR analysis.

Quantitative RT-PCR

Fourth instar nymphs of BPH were treated with EB after which total RNA was extracted from 5th instar nymphs and 1-7 day post-eclosion females of *N. lugens* using the methods detailed above. The HiScript® II RT SuperMix for qPCR (+gDNA wiper) kit from Vazyme, Nanjing, China, was used to create first-strand cDNA. Primer3 (http://bioinfo.ut.ee/primer3/) was used to design real-time quantitative PCR (qPCR) primers listed in Table S2. mRNA levels of candidate genes were detected by qPCR using the UltraSYBR Mixture (with ROX) Kit (CWBIO, Beijing, China). Each reaction contained 2 μL of cDNA template (500 ng), 1 μL each forward and reverse qPCR primer (10 μM), 10 μL of UltraSYBR mixture buffer, and 6 μL of RNase-free water. Q-PCR was run on an ABI 7500 Real-Time PCR System (Applied Biosystems, Foster City, CA) under the following conditions: 5 min at 95°C, followed by 40 cycles of 95°C for 10 s and 60°C for 30 s. Three independent biological replicates and four technical replicates were used in each qPCR experiment. The housekeeping gene 18S ribosomal RNA was used to normalize the expression of candidate genes. The $2^{-\Delta\Delta Ct}$ method (Ct represents the cycle threshold) was used to measure relative expression levels (Livak and Schmittgen, 2001). Three biological replicates were used for statistical comparison between samples. Table S2 contains a list of the primers used in this study.

Gene expression quantification following RNAi.

In late fourth-instar nymphs, we injected 40 nl of synthesized dsRNA targeting *GFP*, *JHAMT*, or *Kr-h1* (5,000 ng/μl). After a 24-hour recovery period, we applied emamectin benzoate (EB) using the systemic route described previously, while control rice seedlings were treated with a 0.1% Triton X-100 aqueous solution. Seventy-two hours post-treatment, we collected female brown planthoppers from each treatment group (at least four groups, n ≥ 5 per group) for total RNA extraction and first-strand cDNA synthesis. We then performed qPCR to measure mRNA levels of the candidate genes *JHAMT* and *Kr-h1* using the UltraSYBR Mixture (with ROX) kit (Beijing Zhongwei Biotech Co., China). The primers for dsRNA synthesis and the qPCR primers were identical to those used in the previous experiments.

Statistics

PoloPlus v2.0 (LeOra Sofware 2008) was used to calculate the lethal concentration (LC_{50}) and 95% fiducial limits (95% F.L.) from bioassay data. GraphPad Prism 8.0 software (GraphPad Software Inc., San Diego, USA) was used to generate graphs and perform statistical analysis of data. Data presented in this study were first verified for normal distribution using the D'Agostino–Pearson normality test. One-way analysis of variance (ANOVA) with Duncan's multiple range test was used to test differences among multiple groups of normally distributed groups of data. Student's t test was used to test the differences between two groups. If data was not normally distributed, Mann–Whitney tests were used for pairwise comparisons, and Kruskal–Wallis test used for comparisons among multiple groups, followed by Dunn's multiple comparisons. All data are presented in figures as mean ± s.e.m. The sample

sizes and statistical tests used for each experiment are stated in the figures or figure legends.

Table S2 Sequences of oligonucleotide primers used in this study.

Primers	Primer sequences (5' - 3')
For cDNA cloning	
Allatotropin：	
NlAT-F	TACGCGGCCAAACACACTTA
NlAT-R	AGGGAAAGAGGGCGAAATTCA
Allatostatins：	
NlAstA-F	TCGGCCGTCACAAGTCAAG
NlAstA-R	CCGAACCCGTACTTCATGCT
NlAstB-F	ACCGGGCTCACAGGAATTTT
NlAstB-R	TGTAGGCGCAGATCTTGAGG
NlAstCC-F	AACACAGCTCTACGAGGCAC
NlAstCC-R	CCAAGCAGGTGACTGCCATA
NlAstCCC-F	TTTGTGTGTGCTTGCAGGTG
NlAstCCC-R	GGATAGAAACGGTAGATTTGGTAGA
Allatostatins receptor：	
NlA16-F	CCTCATTGTGGAACCACCGA
NlA16-R	CGCAGCTGTAAGGTGGAAGA
NlA2-F	GAACGTAATGGGAGTCGGCA
NlA2-R	GTTTTTGTGAGCGCCGACTT
NlA10-F	ATGCAAAACACGGCCAGCCT
NlA10-R	TTAATCGTCTCTGCTCAACTCCAAAGGAAGGT
NlA1-F	CGACCAGACCACTCTACTGC
NlA1-R	ACGTGGACCTCACTATACCAAAAA
For Quantitative RT-PCR	
Q-Nl18S-F	CGCTACTACCGATTGAA
Q-Nl18S-R	GGAAACCTTGTTACGACTT
Q-vitellogenin-F	GTGGCTCGTTCAAGGTTATGG
Q-vitellogenin-R	GCAATCTCTGGGTGCTGTTG
Q-Vitellogenin receptor-F	AGGCAGCCACACAGATAACCGC
Q-Vitellogenin receptor-R	AGCCGCTCGCTCCAGAACATT
Q-JHE-F	GAGCCTCACATCCACAGC
Q-JHE-R	AATGGGAGCCCTACGC
Q-NlMet-F	GGTGGTAAACGGATTGGAAA
Q-NlMet-R	CATCGTCAGCCAACTCGATA
Q-JHAMT-F	GAACCTGCAGGCCAAACACA
Q-JHAMT-R	ACCACTCGGTTGGGCTGAAT

Q-NlKr-h1-F	TGATGAGGCACACGATGACT
Q-NlKr-h1-R	ATGGAAGGCCACATCAAGAG
Q-NlAT-F	CACGATACGTGGCTTCAAGA
Q-NlAT-R	ACGATCACTTTCGCCAATTC
Q-NlAstA-F	AGGACTTACTGGGCGAGGAT
Q-NlAstA-R	GGTGTCTCGTTTCCTGGTGT
Q-NlAstB-F	AGCGAGCTAGACGAGGACAA
Q-NlAstB-R	TCGTCTCTGCTCAACTCCAA
Q-NlAstCC-F	CTGCTCCCAGTGAAAAGGAG
Q-NlAstCC-R	GCTTCCAGTAACTGCGCTTC
Q-NlAstCCC-F	TGTGCTTGCAGGTGGTAGTC
Q-NlAstCCC-F	AGAAGCATGTGACTGCGTTG
Q-NlA2-F	TCCTGGTGCTGAAGAGTGTG
Q-NlA2-R	CTTTTCGGGCCCATTAATTT
Q-NLA1-F	ATATCGGCACCGAAGATGAG
Q-NLA1-R	GTCTGACCCGACAGGTTCTC
Q-NLA10-F	ACTGGGTGTCGACCAATCTC
Q-NLA10-R	TCGGTAGCGAGGAAGACAGT
Q-NLA16-F	TACCGTTCTGTGGGATGTCA
Q-NLA16-R	CCGGGATATCAAAGACGAGA
Q-NlGluCl-F	CACTGACTGAGGCCAACAGA
Q-NlGluCl-R	GCTGGCCATTCTTAGTGAGC

For double-stranded RNA synthesis

T7-EGFP-F	TAATACGACTCACTATAGGGCGTAAACGGCCACAAGTTCA
T7-EGFP-R	TAATACGACTCACTATAGGGGACTGGGTGCTCAGGTAGTG
T7-Kr-h1-F	TAATACGACTCACTATAGGGCGCCAGTGAAAGTGAGACCT
T7-Kr-h1-R	TAATACGACTCACTATAGGGGAGACCGCAAGTGGTTCTGA
T7-Met-F	TAATACGACTCACTATAGGGCCACCAACCAGCAGATGAACCTGA
T7-Met-R	TAATACGACTCACTATAGGGCCACGCAAAGCCTCGTACTCTTGG
T7-JHAMT-F	TAATACGACTCACTATAGGGCTCCAGGCCATTGTCCCTCA
T7-JHAMT-R	TAATACGACTCACTATAGGGTTGGCCTGCAGGTTCTTTGG
T7-AstA-R-F	TAATACGACTCACTATAGGGTACTGCCGTTCTGGCCTTTT
T7-AstA-R-R	TAATACGACTCACTATAGGGGTGATCTGGAAGAGCGGCTT
T7-Glucl-F	TAATACGACTCACTATAGGGACACATCACCTGCTCACCTG
T7-Glucl-R	TAATACGACTCACTATAGGGGTGTGTTTGCCTGCTGTCTG

Acknowledgments

This research was funded by the National Key R&D Program of China to SFW (2022YFD1700200) (https://service.most.gov.cn/) and National Natural Science Foundation of China to SFW (32472542) (https://www.nsfc.gov.cn/). The funders had no role in study design, data collection and analysis, decision to publish, or preparation of the manuscript.

References

Ahmed, T.H., Saunders, T.R., Mullins, D., Rahman, M.Z., Zhu, J., 2020. Molecular action of pyriproxyfen: Role of the Methoprene-tolerant protein in the pyriproxyfen-induced sterilization of adult female mosquitoes. PLoS Negl Trop Dis. 14, e0008669.

Amezian, D., Fricaux, T., de Sousa, G., Maiwald, F., Huditz, H.-I., Nauen, R., Le Goff, G., 2023. Investigating the role of the ROS/CncC signaling pathway in the response to xenobiotics in Spodoptera frugiperda using Sf9 cells. Pesticide Biochemistry and Physiology 195, 105563.

Audsley, N., Vandersmissen, H.P., Weaver, R., Dani, P., Matthews, J., Down, R., Vuerinckx, K., Kim, Y.-J., Vanden Broeck, J., 2013. Characterisation and tissue distribution of the PISCF allatostatin receptor in the red flour beetle, *Tribolium castaneum*. Insect Biochem Mol Biol. 43, 65-74.

Badisco, L., Van Wielendaele, P., Vanden Broeck, J., 2013. Eat to reproduce: a key role for the insulin signaling pathway in adult insects. Frontiers in Physiology Volume 4 - 2013.

Bellés, X., Graham, L.A., Bendenab, W.G., Ding, Q., Edwards, J.P., Weaver, R.J., Tobe, S.S., 1999. The molecular evolution of the allatostatin precursor in cockroaches. Peptides 20, 11-22.

Bownes, M., Rembold, H., 1987. The titre of juvenile hormone during the pupal and adult stages of the life cycle of *Drosophila melanogaster*. Eur J Biochem. 164, 709-712.

Charles, J.-P., Iwema, T., Epa, V.C., Takaki, K., Rynes, J., Jindra, M., 2011. Ligand-binding properties of a juvenile hormone receptor, Methoprene-tolerant. Proceedings of the National Academy of Sciences 108, 21128.

Chen, B., Wen, L., Zhao, J., Liang, H., Jiao, X., 2017. Laboratory risk assessment of seven insecticides to the wolf spider *Pardosa pseudoannulata*. J. Plant Protect. 44, 1059-1060.

Cheng, J., Huang, L.-J., Zhu, Z.-F., Jiang, L.-B., Ge, L.-Q., Wu, J.-C., 2014. Heat-dependent fecundity enhancement observed in *Nilaparvata lugens* (Hemiptera: Delphacidae) after treatment with triazophos. Environ Entomol. 43, 474-481.

Chiang, A.-S., Lin, W.-Y., Liu, H.-P., Pszczolkowski, M.A., Fu, T.-F., Chiu, S.-L., Holbrook, G.L., 2002a. Insect NMDA receptors mediate juvenile hormone biosynthesis. Proceedings of the National Academy of Sciences 99, 37.

Chiang, A.-S., Pszczolkowski, M.A., Liu, H.-P., Lin, S.-C., 2002b. Ionotropic glutamate receptors mediate juvenile hormone synthesis in the cockroach, *Diploptera punctata*. Insect Biochemistry and Molecular Biology 32, 669-678.

Chintalapati, P., Katti, G., Puskur, R.R., Nagella Venkata, K., 2016. Neonicotinoid-induced resurgence of rice leaffolder, *Cnaphalocrocis medinalis* (Guénee). Pest Manag. Sci. 72, 155-161.

Du, B., Ding, D., Ma, C., Guo, W., Kang, L., 2022. Locust density shapes energy metabolism and oxidative stress resulting in divergence of flight traits. Proc Natl Acad Sci U S A. 119, e2115753118.

Fu, B., Liang, J., Hu, J., Du, T., Tan, Q., He, C., Wei, X., Gong, P., Yang, J., Liu, S., Huang, M., Gui, L., Liu, K., Zhou, X., Nauen, R., Bass, C., Yang, X., Zhang, Y., 2024. GPCR–MAPK signaling pathways underpin fitness trade-offs in whitefly. Proceedings of the National Academy of Sciences 121, e2402407121.

Gandara, L., Jacoby, R., Laurent, F., Spatuzzi, M., Vlachopoulos, N., Borst, N.O., Ekmen, G., Potel, C.M., Garrido-Rodriguez, M., Böhmert, A.L., Misunou, N., Bartmanski, B.J., Li, X.C., Kutra, D., Hériché, J.-K., Tischer, C., Zimmermann-Kogadeeva, M., Ingham, V.A., Savitski, M.M., Masson, J.-B., Zimmermann, M., Crocker, J., 2024. Pervasive sublethal effects of agrochemicals on insects at environmentally relevant concentrations. Science 386, 446-453.

Ge, L.-Q., Cheng, Y., Wu, J.-C., Jahn, G.C., 2011. Proteomic analysis of insecticide triazophos-induced mating-responsive proteins of *Nilaparvata lugens* Stål (Hemiptera: Delphacidae). J. Proteome Res. 10, 4597-4612.

Ge, L.-Q., Huang, L.-J., Yang, G.-Q., Song, Q.-S., Stanley, D., Gurr, G.M., Wu, J.-C., 2013. Molecular basis for insecticide-enhanced thermotolerance in the brown planthopper *Nilaparvata lugens* Stål (Hemiptera:Delphacidae). Mol. Ecol. 22, 5624-5634.

Ge, L.-Q., Wu, J.-C., Zhao, K.-F., Chen, Y., Yang, G.-Q., 2010. Induction of Nlvg and suppression of Nljhe gene expression in *Nilaparvata lugens* (Stål) (Hemiptera: Delphacidae) adult females and males exposed to two insecticides. Pestic. Biochem. Physiol. 98, 269-278.

Gospocic, J., Glastad, K.M., Sheng, L., Shields, E.J., Berger, S.L., Bonasio, R., 2021. Kr-h1 maintains distinct caste-specific neurotranscriptomes in response to socially regulated hormones. Cell 184, 5807-5823.e5814.

Guedes, R.N.C., Smagghe, G., Stark, J.D., Desneux, N., 2016. Pesticide-induced stress in arthropod pests for optimized integrated pest management programs. Annu Rev Entomol. 61, 43-62.

Guo, W., Song, J., Yang, P., Chen, X., Chen, D., Ren, D., Kang, L., Wang, X., 2020. Juvenile hormone suppresses aggregation behavior through influencing antennal gene expression in locusts. PLoS Genet. 16, e1008762.

Hardin, M.R., Benrey, B., Coll, M., Lamp, W.O., Roderick, G.K., Barbosa, P., 1995. Arthropod pest resurgence: an overview of potential mechanisms. Crop Protection 14, 3-18.

Hasebe, M., Shiga, S., 2022. Clock gene-dependent glutamate dynamics in the bean bug brain regulate photoperiodic reproduction. PLOS Biol. 20, e3001734.

Hentze, J.L., Carlsson, M.A., Kondo, S., Nässel, D.R., Rewitz, K.F., 2015. The neuropeptide allatostatin A regulates metabolism and feeding decisions in *Drosophila*. Sci. Rep. 5, 11680.

Hu, B., Huang, H., Hu, S., Ren, M., Wei, Q., Tian, X., Esmail Abdalla Elzaki, M., Bass, C., Su, J., Reddy Palli, S., 2021. Changes in both trans- and cis-regulatory elements mediate insecticide resistance in a lepidopteron pest, Spodoptera exigua. PLOS Genetics 17, e1009403.

Huang, J.M., Rao, C., Wang, S., He, L.F., Zhao, S.Q., Zhou, L.Q., Zhao, Y.X., Yang, F.X., Gao, C.F., Wu, S.F., 2020. Multiple target-site mutations occurring in lepidopterans confer resistance to diamide insecticides. Insect Biochem. Mol. Biol. 121, 103367.

Hun, L.V., Okamoto, N., Imura, E., Maxson, R., Bittar, R., Yamanaka, N., 2022. Essential functions of mosquito ecdysone importers in development and reproduction. Proc Natl Acad Sci U S A. 119, e2202932119.

Ishaaya, I., Kontsedalov, S., Horowitz, A.R., 2002. Emamectin, a novel insecticide for controlling field crop pests. Pest Manag. Sci. 58, 1091-1095.

Janssen, A., van Rijn, P.C.J., 2021. Pesticides do not significantly reduce arthropod pest densities in the presence of natural enemies. Ecol Lett. 24, 2010-2024.

Jiang, H., Meng, X., Zhang, N., Ge, H., Wei, J., Qian, K., Zheng, Y., Park, Y., Reddy Palli, S., Wang, J., 2023. The pleiotropic AMPK–CncC signaling pathway regulates the trade-off between detoxification and reproduction. Proceedings of the National Academy of Sciences 120, e2214038120.

Jin, M.-n., Xue, J., Yao, Y., Lin, X.-d., 2014. Molecular characterization and functional analysis of krüppel-homolog 1 (Kr-h1) in the brown planthopper, *Nilaparvata lugens* (Stål). J Integr Agric. 13, 1972-1981.

Jindra, M., Palli, S.R., Riddiford, L.M., 2013. The juvenile hormone signaling pathway in insect development. Annu Rev Entomol. 58, 181-204.

Jindra, M., Uhlirova, M., Charles, J.-P., Smykal, V., Hill, R.J., 2015. Genetic evidence for function of the bHLH-PAS p[rotein Gce/Met as a juvenile hormone receptor. PLOS Genetics 11, e1005394.

Jing, Y.-P., Wen, X., Li, L., Zhang, S., Zhang, C., Zhou, S., 2021. The vitellogenin receptor functionality of the migratory locust depends on its phosphorylation by juvenile hormone. Proc Natl Acad Sci U S A. 118, e2106908118.

Kamita, S.G., Hinton, A.C., Wheelock, C.E., Wogulis, M.D., Wilson, D.K., Wolf, N.M., Stok, J.E., Hock, B., Hammock, B.D., 2003. Juvenile hormone (JH) esterase: why are you so JH specific? Insect Biochem Mol Biol. 33, 1261-1273.

Kataoka, H., Toschi, A., Li, J.P., Carney, R.L., Schooley, D.A., Kramer, S.J., 1989. Identification of an allatotropin from adult *Manduca Sexta*. Science 243, 1481-1483.

Ko, K.I., Root, C.M., Lindsay, S.A., Zaninovich, O.A., Shepherd, A.K., Wasserman, S.A., Kim, S.M., Wang, J.W., 2015. Starvation promotes concerted modulation of appetitive olfactory behavior via parallel neuromodulatory circuits. eLife 4, e08298.

Kramer, S.J., Toschi, A., Miller, C.A., Kataoka, H., Quistad, G.B., Li, J.P., Carney, R.L., Schooley, D.A., 1991. Identification of an allatostatin from the tobacco hornworm *Manduca sexta*. Proc Natl Acad Sci U S A. 88, 9458-9462.

Lin, X., Yao, Y., Wang, B., 2015. Methoprene-tolerant (Met) and Krüpple-homologue 1 (Kr-h1) are required for ovariole development and egg maturation in the brown plant hopper. Sci. Rep. 5, 18064.

Ling, L., Raikhel, A.S., 2018. Serotonin signaling regulates insulin-like peptides for growth, reproduction, and metabolism in the disease vector *Aedes aegypti*. Proc Natl Acad Sci U S A. 115, E9822.

Ling, L., Raikhel, A.S., 2021. Cross-talk of insulin-like peptides, juvenile hormone, and 20-hydroxyecdysone in regulation of metabolism in the mosquito *Aedes aegypti*. Proc. Natl. Acad. Sci. U S A. 118, e2023470118.

Liu, H.-P., Lin, S.-C., Lin, C.-Y., Yeh, S.-R., Chiang, A.-S., 2005. Glutamate-gated chloride channels inhibit juvenile hormone biosynthesis in the cockroach, *Diploptera punctata*. Insect Biochem Mol Biol. 35, 1260-1268.

Liu, S., Ding, Z., Zhang, C., Yang, B., Liu, Z., 2010a. Gene knockdown by intro-thoracic injection of double-stranded RNA in the brown planthopper, Nilaparvata lugens. Insect Biochem. Mol. Biol. 40, 666-671.

Liu, S., Zhang, C., Yang, B., Gu, J., Liu, Z., 2010b. Cloning and characterization of a putative farnesoic acid O -methyltransferase gene from the brown planthopper, *Nilaparvata lugens*. J Insect Sci. 10.

Livak, K.J., Schmittgen, T.D., 2001. Analysis of relative gene expression data using real-time quantitative PCR and the $2^{-\Delta\Delta CT}$ method. Methods 25, 402-408.

Lorenz, M.W., Kellner, R., Hoffmann, K.H., 1995. A family of neuropeptides that inhibit juvenile hormone biosynthesis in the cricket, *Gryllus bimaculatus*. J. Biol. Chem. 270, 21103-21108.

Lu, K., Chen, X., Liu, W.-T., Zhou, Q., 2016. TOR pathway-mediated juvenile hormone synthesis regulates nutrient-dependent female reproduction in *Nilaparvata lugens* (Stål). Int. J. Mol. Sci. 17, 438.

Luo, W., Liu, S., Zhang, W., Yang, L., Huang, J., Zhou, S., Feng, Q., Palli, S.R., Wang, J., Roth, S., Li, S., 2021. Juvenile hormone signaling promotes ovulation and maintains egg shape by inducing expression of extracellular matrix genes. Proc. Natl. Acad. Sci. U S A. 118, e2104461118.

Meiselman, M.R., Alpert, M.H., Cui, X., Shea, J., Gregg, I., Gallio, M., Yapici, N., 2022. Recovery from cold-induced reproductive dormancy is regulated by temperature-dependent AstC signaling. Current Biol. 32, 1362-1375.e1368.

Mirth, C.K., Tang, H.Y., Makohon-Moore, S.C., Salhadar, S., Gokhale, R.H., Warner, R.D., Koyama, T., Riddiford, L.M., Shingleton, A.W., 2014. Juvenile hormone regulates body size and perturbs insulin signaling in *Drosophila*. Proceedings of the National Academy of Sciences 111, 7018-7023.

Nässel, D.R., 2002. Neuropeptides in the nervous system of *Drosophila* and other insects: multiple roles as neuromodulators and neurohormones. Prog Neurobiol. 68, 1-84.

Nouzova, M., Rivera-Pérez, C., Noriega, F.G., 2018. Omics approaches to study juvenile hormone synthesis. Curr Opin Insect Sci. 29, 49-55.

Peng, Y.C., Sheng, C.W., Casida, J.E., Zhao, C.Q., Han, Z.J., 2017. Ryanodine receptor genes of the rice stem borer, *Chilo suppressalis*: Molecular cloning, alternative splicing and expression profiling. Pestic. Biochem. Physiol. 135, 69-77.

Riddiford, L.M., 2008. Juvenile hormone action: A 2007 perspective. J Insect Physiol. 54, 895-901.

Riddiford, L.M., 2020. Rhodnius, golden oil, and met: A history of juvenile hormone research. Front Cell Dev Biol. 8.

Root, Cory M., Ko, Kang I., Jafari, A., Wang, Jing W., 2011. Presynaptic facilitation by neuropeptide signaling mediates odor-driven food search. Cell 145, 133-144.

Roy, S., Saha, T.T., Johnson, L., Zhao, B., Ha, J., White, K.P., Girke, T., Zou, Z., Raikhel, A.S., 2015. Regulation of gene expression patterns in mosquito reproduction. PLoS Genet. 11, e1005450.

Santos, C.G., Humann, F.C., Hartfelder, K., 2019. Juvenile hormone signaling in insect oogenesis. Curr Opin Insect Sci. 31, 43-48.

Shah, S., Zhang, S.-S., Elgizawy, K.K., Yan, W.-H., Tang, N., Wu, G., Yang, F.-L., 2022. Diallyl trisulfide reduced the reproductive capacity of male *Sitotroga cerealella* via the regulation of juvenile and ecdysone hormones. Ecotoxicol. Environ. Saf. 248, 114304.

Shen, Y., Chen, Y.-Z., Lou, Y.-H., Zhang, C.-X., 2019. Vitellogenin and vitellogenin-like genes in the brown planthopper. Front Physiol. 10.

Sheng, Z., Xu, J., Bai, H., Zhu, F., Palli, S.R., 2011. Juvenile hormone regulates vitellogenin gene expression through insulin-like peptide signaling pathway in the red flour beetle, *Tribolium castaneum*. Journal of Biological Chemistry 286, 41924-41936.

Shinoda, T., Itoyama, K., 2003. Juvenile hormone acid methyltransferase: A key regulatory enzyme for insect metamorphosis. Proc Natl Acad Sci U S A. 100, 11986.

Smykal, V., Raikhel, A.S., 2015. Nutritional control of insect reproduction. Curr Opin Insect Sci. 11, 31-38.

Sogawa, K., 2015. Planthopper outbreaks in different paddy ecosystems in Asia: Man-made hopper plagues that threatened the green revolution in rice, in: Heong, K.L., Cheng, J., Escalada, M.M. (Eds.), Rice Planthoppers: Ecology, Management, Socio Economics and Policy. Springer Netherlands, Dordrecht, pp. 33-63.

Sōgawa, K., 1982. The rice brown planthopper: Feeding physiology and host plant interactions. Annu Rev Entomol. 27, 49-73.

Sparks, T.C., Crossthwaite, A.J., Nauen, R., Banba, S., Cordova, D., Earley, F., Ebbinghaus-Kintscher, U., Fujioka, S., Hirao, A., Karmon, D.,

Kennedy, R., Nakao, T., Popham, H.J.R., Salgado, V., Watson, G.B., Wedel, B.J., Wessels, F.J., 2020. Insecticides, biologics and nematicides: Updates to IRAC's mode of action classification - a tool for resistance management. Pestic. Biochem. Physiol. 167, 104587.

Sparks, T.C., Storer, N., Porter, A., Slater, R., Nauen, R., 2021. Insecticide resistance management and industry: the origins and evolution of the Insecticide Resistance Action Committee (IRAC) and the mode of action classification scheme. Pest Manag. Sci. 77, 2609-2619.

Stay, B., Fairbairn, S., Yu, C.G., 1996. Role of allatostatins in the regulation of juvenile hormone synthesis. Arch Insect Biochem Physiol. 32, 287-297.

Stay, B., Tobe, S.S., 2007. The role of allatostatins in juvenile hormone synthesis in insects and crustaceans. Annu Rev Entomol. 52, 277-299.

Tamura, K., Stecher, G., Peterson, D., Filipski, A., Kumar, S., 2013. MEGA6: Molecular evolutionary genetics analysis version 6.0. Mol Biol Evol. 30, 2725-2729.

Tanaka, Y., Suetsugu, Y., Yamamoto, K., Noda, H., Shinoda, T., 2014. Transcriptome analysis of neuropeptides and G-protein coupled receptors (GPCRs) for neuropeptides in the brown planthopper *Nilaparvata lugens*. Peptides 53, 125-133.

Veenstra, J.A., 2009. Allatostatin C and its paralog allatostatin double C: The arthropod somatostatins. Insect Biochem Mol Biol. 39, 161-170.

Veenstra, J.A., 2016. Allatostatins C, double C and triple C, the result of a local gene triplication in an ancestral arthropod. Gen Comp Endocrinol. 230-231, 153-157.

Verlinden, H., Gijbels, M., Lismont, E., Lenaerts, C., Vanden Broeck, J., Marchal, E., 2015. The pleiotropic allatoregulatory neuropeptides and their receptors: A mini-review. J Insect Physiol. 80, 2-14.

Wan, D.-J., Chen, J., Jiang, L.-B., Ge, L.-Q., Wu, J.-C., 2013. Effects of the insecticide triazophos on the ultrastructure of the flight muscle of the brown planthopper *Nilaparvata lugens* Stål (Hemiptera: Delphacidae). Crop Protection 43, 54-59.

Wang, C., Chin-Sang, I., Bendena, W.G., 2012. The FGLamide-Allatostatins influence foraging behavior in *Drosophila melanogaster*. PLOS ONE 7, e36059.

Wang, G., Vega-Rodríguez, J., Diabate, A., Liu, J., Cui, C., Nignan, C., Dong, L., Li, F., Ouedrago, C.O., Bandaogo, A.M., Sawadogo, P.S., Maiga, H., Alves e Silva, T.L., Pascini, T.V., Wang, S., Jacobs-Lorena, M., 2021. Clock genes and environmental cues coordinate *Anopheles* pheromone synthesis, swarming, and mating. Science 371, 411.

Wang, L.-P., Shen, J., Ge, L.-Q., Wu, J.-C., Yang, G.-Q., Jahn, G.C., 2010. Insecticide-induced increase in the protein content of male accessory glands and its effect on the fecundity of females in the brown planthopper *Nilaparvata lugens* Stål (Hemiptera: Delphacidae). Crop Protection 29, 1280-1285.

Wegener, C., Chen, J., 2022. Allatostatin A signalling: Progress and new challenges from a paradigmatic pleiotropic invertebrate neuropeptide family. Front Physiol. 13.

Wolstenholme, A.J., 2012. Glutamate-gated Chloride Channels *. Journal of Biological Chemistry 287, 40232-40238.

Woodhead, A.P., Stay, B., Seidel, S.L., Khan, M.A., Tobe, S.S., 1989. Primary structure of four allatostatins: neuropeptide inhibitors of juvenile hormone synthesis. Proc Natl Acad Sci U S A. 86, 5997-6001.

Wu, J., Ge, L., Liu, F., Song, Q., Stanley, D., 2020. Pesticide-induced planthopper population resurgence in rice cropping systems. Annu Rev Entomol. 65, 409-429.

Wu, S.F., Ja, Y.L., Zhang, Y.J., Yang, C.H., 2019. Sweet neurons inhibit texture discrimination by signaling TMC-expressing mechanosensitive neurons in *Drosophila*. eLife 8, e46165.

Wu, S.F., Mu, X.C., Dong, Y.X., Wang, L.X., Wei, Q., Gao, C.F., 2017. Expression pattern and pharmacological characterisation of two novel alternative splice variants of the glutamate-gated chloride channel in the small brown planthopper *Laodelphax striatellus*. Pest Manag. Sci. 73, 590-597.

Wu, S.F., Zeng, B., Zheng, C., Mu, X.C., Zhang, Y., Hu, J., Zhang, S., Gao, C.F., Shen, J.L., 2018a. The evolution of insecticide resistance in the brown planthopper (*Nilaparvata lugens* Stål) of China in the period 2012–2016. Sci. Rep. 8, 4586.

Wu, Y., Ding, J., Xu, B., You, L., Ge, L., Yang, G., Liu, F., Stanley, D., Song, Q., Wu, J., 2018b. Two fungicides alter reproduction of the small brown planthopper *Laodelphax striatellus* by influencing gene and protein expression. J Proteome Res. 17, 978-986.

Xu, B., You, L.-L., Wu, Y., Ding, J., Ge, L.-Q., Wu, J.-C., 2016. Transmission electron microscopy (TEM) observations of female oocytes from *Nilaparvata lugens* (Hemiptera: Delphacidae): Antibiotic jinggangmycin (JGM)-induced stimulation of reproduction and associated

changes in hormone levels. J Econ Entomol. 109, 1677-1682.

Xu, H.J., Xue, J., Lu, B., Zhang, X.C., Zhuo, J.C., He, S.F., Ma, X.F., Jiang, Y.Q., Fan, H.W., Xu, J.Y., Ye, Y.X., Pan, P.L., Li, Q., Bao, Y.Y., Nijhout, H.F., Zhang, C.X., 2015. Two insulin receptors determine alternative wing morphs in planthoppers. Nature advance online publication.

Yagi, K.J., Kwok, R., Chan, K.K., Setter, R.R., Myles, T.G., Tobe, S.S., Stay, B., 2005. Phe-Gly-Leu-amide allatostatin in the termite *Reticulitermes flavipes*: Content in brain and corpus allatum and effect on juvenile hormone synthesis. J Insect Physiol. 51, 357-365.

Yang, H., Zhou, C., Jin, D.-c., Gong, M.-f., Wang, Z., Long, G.-y., 2019. Sublethal effects of abamectin on the development, fecundity, and wing morphs of the brown planthopper *Nilaparvata lugens*. J Asia Pac Entomol. 22, 1180-1186.

Yao, R., Zhao, D.D., Zhang, S., Zhou, L.Q., Wang, X., Gao, C.F., Wu, S.F., 2017. Monitoring and mechanisms of insecticide resistance in *Chilo suppressalis* (Lepidoptera: Crambidae), with special reference to diamides. Pest Manag. Sci. 73, 1169-1178.

Yin, G.-L., Yang, J.-S., Cao, J.-X., Yang, W.-J., 2006. Molecular cloning and characterization of FGLamide allatostatin gene from the prawn, *Macrobrachium rosenbergii*. Peptides 27, 1241-1250.

Yin, J.-L., Xu, H.-W., Wu, J.-C., Hu, J.-H., Yang, G.-Q., 2014. Cultivar and insecticide applications affect the physiological development of the brown planthopper, *Nilaparvata lugens* (Stål) (Hemiptera: Delphacidae). Environ Entomol. 37, 206-212.

Zeng, B., Chen, F.-R., Liu, Y.-T., Di, G., Zhang, Y.-J., Feng, Z.-R., Wang, L.-X., Vontas, J., Wu, S.-F., Zhu, K.Y., Gao, C.-F., 2023. A chitin synthase mutation confers widespread resistance to buprofezin, a chitin synthesis inhibitor, in the brown planthopper, *Nilaparvata lugens*. J. Pest Sci. 96, 819–832.

Zhang, C., Daubnerova, I., Jang, Y.-H., Kondo, S., Žitňan, D., Kim, Y.-J., 2021. The neuropeptide allatostatin C from clock-associated DN1p neurons generates the circadian rhythm for oogenesis. Proc Natl Acad Sci U S A. 118, e2016878118.

Zhang, C., Kim, A.J., Rivera-Perez, C., Noriega, F.G., Kim, Y.-J., 2022a. The insect somatostatin pathway gates vitellogenesis progression during reproductive maturation and the post-mating response. Nat Commun. 13, 969.

Zhang, Y.-X., Zhu, Z.-F., Lu, X.-L., Li, X., Ge, L.-Q., Fang, J.-C., Wu, J.-C., 2014. Effects of two pesticides, TZP and JGM, on reproduction of three planthopper species, *Nilaparvata lugens* Stål, *Sogatella furcifera* Horvath, and *Laodelphax striatella* Fallén. Pestic. Biochem. Physiol. 115, 53-57.

Zhang, Y., Ruan, Y., Gong, C., Zhang, S., Zhang, J., He, Y., Wang, Q., Liu, D., Pu, J., Liu, X., Jiang, C., Wang, X., 2022b. Reproductive outbreaks of *Sogatella furcifera* mediated by overexpression of the nuclear receptor USP under pressure from triflumezopyrim. Int J Mol Sci. 23, 13769.

Zhang, Y., Wang, X., Yang, B., Hu, Y., Huang, L., Bass, C., Liu, Z., 2015. Reduction in mRNA and protein expression of a nicotinic acetylcholine receptor α8 subunit is associated with resistance to imidacloprid in the brown planthopper, Nilaparvata lugens. Journal of Neurochemistry 135, 686-694.

Zhao, K.-F., Shi, Z.-P., Wu, J.-C., 2011. Insecticide-induced enhancement of flight capacity of the brown planthopper *Nilaparvata lugens* Stål (Hemiptera: Delphacidae). Crop Protection 30, 476-482.

Zheng, H., Wang, N., Yun, J., Xu, H., Yang, J., Zhou, S., 2022. Juvenile hormone promotes paracellular transport of yolk proteins via remodeling zonula adherens at tricellular junctions in the follicular epithelium. PLoS Genet. 18, e1010292.

Zhu, G.-H., Jiao, Y., Chereddy, S.C.R.R., Noh, M.Y., Palli, S.R., 2019. Knockout of juvenile hormone receptor, Methoprene-tolerant, induces black larval phenotype in the yellow fever mosquito, *Aedes aegypti*. Proc Natl Acad Sci U S A., 201905729.